Aquifer operator scaling and the effect on solute mixing and dispersion

David A. Benson
Geology and Geological Engineering, Colorado School of Mines, Golden, Colorado, USA

Mark M. Meerschaert and Boris Baeumer
Department of Mathematics and Statistics, University of Otago, Dunedin, New Zealand

Hans-Peter Scheffler
Department of Mathematics and Statistics, University of Nevada, Reno, Nevada, USA

Received 21 October 2004; revised 3 October 2005; accepted 13 October 2005; published 25 January 2006.

[1] Since aquifer parameters may have statistical dependence structures that are present across a huge range of scales, the concepts of fractional Brownian motion (fBm) have been used in both analytic and numerical stochastic settings. Most previous models have used isotropic scaling characterized by a single scalar Hurst coefficient. Any real-world anisotropy has been handled by an elliptical stretching random K field. We define a d-dimensional extension of fBm in which the fractional-order integration may take on different orders in the d primary (possibly nonorthogonal) scaling directions, and the degree of connectivity and long-range dependence is freely assigned via a probability measure on the unit sphere. This approach accounts for the different scaling found in the vertical versus horizontal directions in sedimentary aquifers and allows very general degrees of continuity of K in certain directions. It also allows for the representation of fracture networks in a continuum setting: The eigenvectors of the scaling matrix describe the primary fracture scaling directions, and discrete weights of fractional integration represent fracture continuity that may be limited to a small number of directions. In a numerical experiment, the motion of solutes through 2-D ''operator-fractional'' Gaussian fields depends very much on transverse Hurst coefficients. Transverse scaling in the range of fractional Gaussian noise engenders greater plume mixing and a transition to a Fickian regime. Higher orders of integration, in the range of fractional Brownian motion, are associated with thicker layering of aquifer sediments and more preferential, unmixed transport. Therefore direct representation of the unique directional scaling properties of an aquifer is important for realistic simulation of transport.

Citation: Benson, D. A., M. M. Meerschaert, B. Baeumer, and H.-P. Scheffler (2006), Aquifer operator scaling and the effect on solute mixing and dispersion, *Water Resour. Res.*, *42*, W01415, doi:10.1029/2004WR003755.

1. Introduction

[2] Predicting the movement of dissolved chemicals through real-world aquifer material has been a priority of hydrogeologists for decades. In the 1970s, an understanding evolved that no aquifer could be completely characterized [*Freeze*, 1975; *Gelhar et al.*, 1979; *Smith and Schwartz*, 1980]. Uncertain aquifer properties, at every unsampled point, must be represented by some statistical model. Two interrelated methods evolved to model the effect of the uncertain aquifer, using either analytic or numerical methods. The analytic method replaces the deterministic advection-dispersion equation with a stochastic version and solves for the moments of the head and concentration fields (see the extensive review by *Gelhar* [1993]). The numerical approach uses classical Monte Carlo methods [e.g., *Tompson and Gelhar*, 1990], and more recently, Bayesian and other conditioning methods [*Woodbury and Ulrych*, 2000; *Feyen et al.*, 2002; *Morse et al.*, 2003; *Huang et al.*, 2004], to simulate a large number of aquifer realizations (some more likely than others), and either analyzes the ensemble statistics of the head and concentration fields or solves the moment equations themselves [*Graham and McLaughlin*, 1989; *Li and McLaughlin*, 1991; *Li et al.*, 2003, 2004; *Guadagnini and Neuman*, 1999a, 1999b, 2001; *Ye et al.*, 2004]. A number of techniques are widely used to generate scalar random field replicas of aquifers for use in the Monte Carlo studies [*Tompson et al.*, 1989; *Deutsch and Journel*, 1992; *Dietrich and Newsam*, 1993; *Robin et al.*, 1993; *Carle and Fogg*, 1997; *Bruining et al.*, 1997; *Hassan et al.*, 1997; *Ruan and McLaughlin*, 1998; *Painter*, 2001; *Lu et al.*, 2003].

[3] Both the analytic and numerical methods have enjoyed great success for various subsets of the variety of aquifer types. The strength of the analytic method lies in the simplicity of representing the aquifer statistical characteristics, but is burdened with assumptions needed to gain well

0043-1397/06/2004WR003755$09.00

posedness (closure) of the stochastic equations (see a recent discussion by *Wood et al.* [2003]). The strength of the numerical method lies in the robustness of each deterministic solution, the ability to condition with data from specific locations [e.g., *Dietrich and Newsam*, 1996], and the ability to incorporate any number of uncertain parameters [*Burr et al.*, 1994; *Cushman et al.*, 1995; *Hu et al.*, 1995; *Huang and Hu*, 2001]. Furthermore, the rapid and predictable advancement of computer speed and addressable memory allows the representation of aquifer features from many scales. The downside of the numerical method, aside from the computational time required, is that the aquifer facsimiles must be created according to some defined statistical model that is typically an oversimplification. The chosen model should adhere to the real characteristics of the aquifer, including the statistical dependence structures that might be present across all scales [*Neuman*, 1995; *Molz and Boman*, 1993; *Molz et al.*, 1997].

[4] One early statistical model that parsimoniously accounts for evolving heterogeneity at all scales is a fractional Brownian motion (FBM), since this stochastic process has the property of self-similarity [*Mandelbrot and van Ness*, 1968]. However, true multidimensional FBM is an overly restrictive model for several reasons. First, non-Gaussian increments of K or $\ln(K)$ may be the rule, not the exception. The distribution of K or $\ln(K)$ is typically heavier tailed than a Gaussian [*Eggleston et al.*, 1996; *Painter and Paterson*, 1994; *Painter*, 1996, 2001; *Rasmussen et al.*, 1993; *Liu and Molz*, 1996, 1997; *Benson et al.*, 2001; *Hyun and Neuman*, 2003; *Meerschaert et al.*, 2004; *Aban et al.*, 2006]. Since simple FBM can replicate the long-range K dependence that can account for continual faster-than-Fickian growth rate of plumes [e.g., *Kemblowski and Wen*, 1993; *Neuman*, 1995; *Rajaram and Gelhar*, 1995; *Zhan and Wheatcraft*, 1996; *Bellin et al.*, 1996; *Cushman*, 1997; *Hassan et al.*, 1997; *Di Federico and Neuman*, 1998; *Painter and Mahinthakumar*, 1999], it is still the basis of several simulation techniques that have relaxed the restrictive assumption of Gaussian increments [*Painter*, 2001; *Meerschaert et al.*, 2004]. Second, a more serious drawback of simple FBM is its functional, or scaling isotropy, in which the self-similarity parameter is the same in all directions [*Bonami and Estrade*, 2003]. There is no physical reason that a sedimentary aquifer should have the same scaling properties in the vertical and horizontal directions. Evidence for different scaling of sedimentary rock parameters or stream traces in different directions at several sites is presented by *Hewitt* [1986], *Molz and Boman* [1993], *Sapozhnikov and Foufoula-Georgiu* [1996], *Molz et al.* [1997], *Deshpande et al.* [1997], *Tennekoon et al.* [2003], and *Castle et al.* [2004], among others. In this paper we provide a brief reanalysis of the data collected by the latter researchers. Techniques have been developed that can handle this anisotropy in the scaling or the Hurst coefficients [*Dobrushin*, 1978; *Hudson and Mason*, 1982; *Schertzer and Lovejoy*, 1985, 1987; *Kumar and Foufoula-Georgiou*, 1993; *Mason and Xiao*, 2001; *Bonami and Estrade*, 2003] yet the mathematical character of numerical implementations is still under investigation, since many of the properties of these fields have only recently been worked out in one dimension [*Pipiras and Taqqu*, 2000, 2003].

[5] A third complication is that aquifers may possess strong directionality in the K structure. Continuity within high-K units may be restricted to a small subset of the unit circle in two dimensions or the unit sphere in three dimensions. For example, braided streams deposit gravel in continuous channels with distinct preferential directions associated with the mean transport direction (Figure 1). One can easily calculate the proportion of the channels that lie in any angular interval $d\theta$ and construct a histogram of the stream channel directions (Figure 2). If the high-K portions of an aquifer are deposited within these channels, then we presume that the continuity of the aquifer K should follow the same directional control. For reasons that will become clear in subsequent derivations, we describe the proportion of the stream channel lying in any direction by the so-called mixing measure, or weight function, $M(\theta)$. The histogram of directions (Figure 2) shows the strong preference for flow, hence deposition of similar material, in the direction parallel to the bottom edge of the photograph (0°/180°) and almost none in the ±90° directions. The measure of directional dependence $M(\theta)$ is specific to any given site and should be freely assigned within a statistical model of that site. In this paper we construct random fields on the basis of a convolutional formula that allows a general degree of statistical dependence in any given direction. In this example, only the direction of the channel was measured; therefore the measure in Figure 2 is symmetric with the addition of 180°. When measuring actual K values, the dependence may be nonsymmetric with respect to the downstream direction, since a disturbance in the water flow would be expected to deposit a fining downstream sequence of gravel and sand. For supercritical flow, no random disturbance should be reflected in the sediments in the upstream direction at all. We investigate the influence of directional "causality" in a subsequent section.

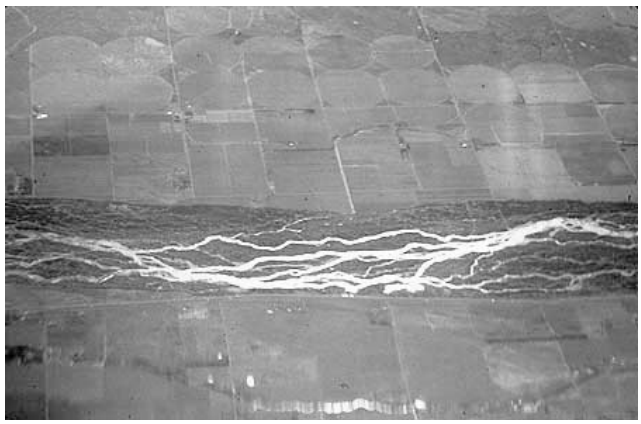

Figure 1. Braided stream channels from above.

[6] Aside from the deposition of sediment grains of various sizes, aquifers may gain permeability structure through deformation. This is particularly important in low-permeability rock, which may acquire fractures that convey essentially all of the groundwater flow. This scenario takes on increased importance, since most of the nations that produce high-level nuclear waste plan to store it within fractured, low-permeability host rock (hence the numerous studies of Yucca Mountain in the United States [*Bodvarsson and Tsang*, 1999; *Bodvarsson*, 2003], and the

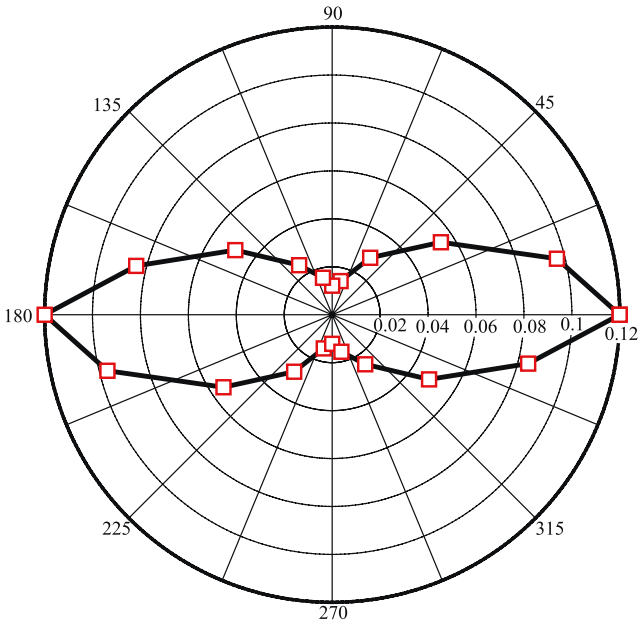

Figure 2. Approximate measure $M(\theta)$ of the directional proportion of the wet portions in Figure 1. Angles are in degrees.

Äspö repository in Sweden [*Swedish Nuclear Fuel and Waste Management (SKB)*, 2001]). Studies of the suitability of these sites [e.g., *Outters and Shuttle*, 2000; *Stigsson et al.*, 2000; *Bechtel SAIC Company (BSC)*, 2004a, 2004b] have endeavored to map the locations of all important fractures and faults that intersect tunnels and drifts. However, the final buildout of the repositories will uncover multitudes of new, as yet unknown fractures, and the regions of rock between the repository and potential receptors will always remain uncharacterized. Some sort of statistical representation of the aquifer (fracture) properties is still needed to supplement the mapping information [*SKB*, 2001, chapter 8]. Real fracture networks are almost universally observed to possess fractal structure (see the extensive review by *Bonnet et al.* [2001]). Permeability measurements in fractured rock also show scale effects and may support fractal models [*Hyun et al.*, 2002; *Neuman and Di Federico*, 2003; *Martinez-Landa and Carrera*, 2005]. The specifics of the more subtle fracture statistics have a large bearing on the transport characteristics of the networks [*Bour and Davy*, 1998; *Bour et al.*, 2003; *Darcel et al.*, 2003a, 2003b; *de Dreuzy et al.*, 2004].

[7] When simulating flow through fracture networks, several approaches can be adopted (see the recent review by *Neuman* [2005a]). The first treats the network, or a subset of the network [e.g., *BSC*, 2004a; *Carrera and Martinez-Landa*, 2000], as an equivalent porous medium (EPM), and derives or measures an effective upscaled K tensor on the basis of the contributions of "subgrid" fractures. The EPM is justified in highly fractured media where the fracture spacing is small compared to some region of interest, say a numerical grid block or the distance between observation points [*Snow*, 1969; *Long et al.*, 1982; *Endo et al.*, 1984; *Hsieh and Neuman*, 1985; *Hsieh et al.*, 1985; *Neuman et al.*, 1984; *Neuman*, 2005b]. However, when the fracture spacing is large compared to the region of interest, then an effective parameter does not reasonably represent the subgrid features (as measured by either flow or heads; see *Wellman and Poeter* [2005]). In this case, the individual fractures, and perhaps as importantly the intervening impermeable rock, may need to be explicitly represented. This can be done using discrete fracture networks [*Adler and Thovert*, 1999; *Benke and Painter*, 2003; *Cvetkovic et al.*, 2004], or by accepting as an approximation a continuous random field, preferably with conditioning on the locations of fractures. One must accept that a continuous random field might assign some regions of impermeable rock a positive definite K tensor, which assumes sufficiently dense subgrid fractures. In the case of fractal networks, there may not be a convenient separation of scales such that individual fractures can be ignored in favor of an equivalent porous medium [*Long et al.*, 1982]. In this paper, we show that a random field, based on an extension of FBM, can represent fractal fracture permeability and preserve fracture orientations and unique scaling properties in different directions. As a result, no separation of scales is invoked to divide the domain into large mappable fractures and subgrid features that constitute an equivalent porous medium. Furthermore, if fractures orientations are concentrated in a few directions, the generation of a continuous random field should be able to restrict the continuity of high-K areas to those directions, as opposed to the more isotropic prior definitions of FBM.

[8] To expand the capabilities of current generators of continuous random fields including classical FBM, we introduce operator-scaling scalar random field generators based on multidimensional fractional integration. The random fields have "operator scaling" that is described by a matrix of values—the linear operator—instead of a single scalar Hurst coefficient. The matrix-valued, or operator rescaling properties mean that the scaling indices (for example, Hurst coefficients for Gaussian fields) can be different in each coordinate. For maximal generality, we choose a fractional integration on the basis of the inverse of the recently defined anisotropic fractional Laplacian [*Meerschaert et al.*, 2001]. The fields we describe in this paper allow all of the following: (1) self-similar structure at all scales, particularly when the scaling rates are unique in different directions, (2) arbitrary strength of statistical dependence along discrete directions, and (3) generality in choosing the statistical distribution of the scalar random field, including nonstationarity. Finally, in section 3, we investigate the influence of simple operator-scaling K structure in synthetic aquifers on the transport of solutes and compare the results to previous stochastic analytic predictions.

2. Mathematical Background

[9] The first d-dimensional FBM $B_H(\mathbf{x})$ was defined as an isotropic special case of the moving average

$$B_\varphi(\mathbf{x}) = \int [\varphi(\mathbf{x}-\mathbf{y}) - \varphi(-\mathbf{y})] B(d\mathbf{y}), \qquad (1)$$

with $B(d\mathbf{y})$ the increment of a Brownian random field, $\varphi(\mathbf{y}) = \|\mathbf{y}\|^{H-d/2}$, and Hurst index $0 < H < 1$ [*Samorodnitsky and Taqqu*, 1994; *Cushman*, 1997]. The first term in the integral is the convolution kernel, which mathematically spreads the

random value at each point over space. The second term centers the motion so that $B_\varphi(\mathbf{0}) = 0$. The stochastic integral $I(f) = \int f(\mathbf{y})B(d\mathbf{y})$ is the distributional limit of approximating sums $\sum_j f(\mathbf{y}_j)B(\Delta\mathbf{y}_j)$ where $\Delta\mathbf{y}_j$ is a small d-dimensional rectangle, $\mathbf{y}_j$ is a point inside that rectangle, $B(\Delta\mathbf{y}_j)$ is a normal random variable with mean zero and variance equal to the volume of that rectangle, and these normal random variables are independent for disjoint rectangles. A finite sum gives a faithful approximation so long as the area covered spreads over entire space as the mesh of the partition tends to zero. The integral $I(f)$ is a mean zero normal random variable with variance proportional to $\int f(\mathbf{y})^2 d\mathbf{y}$, and the integral exists so long as $\int f(\mathbf{y})^2 d\mathbf{y} < \infty$ [e.g., *Yaglom*, 1987]. In this case we say that the function $f(\mathbf{y})$ is square integrable. Since the volume of $c\Delta\mathbf{y}_j$ is c^d times the volume of $\Delta\mathbf{y}_j$, and using the formula $\mathrm{VAR}(aZ) = a^2\mathrm{VAR}(Z)$ for random variables Z, $B(cd\mathbf{y}) = c^{d/2}B(d\mathbf{y})$ in distribution for any scale $c > 0$, and then it follows immediately from (1) that an isotropic fractional Brownian field is self-similar: $B_H(c\mathbf{x}) = c^H B_H(\mathbf{x})$ in distribution. The restriction $0 < H < 1$ comes from the requirement that the integrand in (1) is square integrable. Fractional Gaussian noise is a stationary discrete parameter process obtained by taking differences of a fractional Brownian field, $G_H(j) = B_H(j) - B_H(j-1)$ in one dimension or the corresponding analogue in d dimensions: $G_H(i,j) = B_H(i,j) - B_H(i,j-1) - B_H(i-1,j) + B_H(i-1,j-1)$ in two dimensions and so forth. The noise process inherits the same scaling: $G_H(c\mathbf{x}) = c^H G_H(\mathbf{x})$.

[10] The spectral representation of the Brownian random field (1) is given by

$$B_\varphi(\mathbf{x}) = \int \left[e^{i\mathbf{k}\cdot\mathbf{x}} - 1\right]\hat{\varphi}(\mathbf{k})\hat{B}(d\mathbf{k}), \tag{2}$$

where $\hat{\varphi}(\mathbf{k}) = (2\pi)^{-d/2}\int e^{-i\mathbf{k}\cdot\mathbf{y}}\varphi(\mathbf{y})d\mathbf{y}$. In the isotropic case, $\hat{\varphi}(\mathbf{k}) = C_H\|\mathbf{k}\|^{-H-d/2}$ and $C_H > 0$ is a constant depending only on H and d. The stochastic integral $\int g(\mathbf{k})\hat{B}(d\mathbf{k})$ is the distributional limit of approximating sums $\sum_\ell g(\mathbf{k}_\ell)\hat{B}(\Delta\mathbf{k}_\ell)$ where $\Delta\mathbf{k}_\ell$ is a small d-dimensional rectangle in wave space, and the complex-valued random measure $\hat{B}(\Delta\mathbf{k}_\ell) = m_1(\Delta\mathbf{k}_\ell) + im_2(\Delta\mathbf{k}_\ell)$. The real and complex parts $m_1(\Delta\mathbf{k}_\ell)$ and $m_2(\Delta\mathbf{k}_\ell)$ are independent normal random variables with mean zero and variance equal to half the volume of the rectangle $\Delta\mathbf{k}_\ell$, independent for disjoint rectangles, except that $m_1(\Delta\mathbf{k}_\ell) = m_1(-\Delta\mathbf{k}_\ell)$ and $m_2(\Delta\mathbf{k}_\ell) = -m_2(-\Delta\mathbf{k}_\ell)$ [*Samorodnitsky and Taqqu*, 1994]. The random measure $\hat{B}$ is the Fourier transform of the random measure B in the sense that

$$\hat{B}(\Delta\mathbf{k}_\ell) \approx \frac{1}{\sqrt{N}}\sum_j e^{-i\mathbf{k}_\ell\cdot\mathbf{y}_j}B\left(\Delta\mathbf{y}_j\right), \tag{3}$$

where N is the total number of grid points, the distributional approximation becoming exact as the mesh of the partition tends to zero. The conditions on m_1 and m_2 follow from (3), since this formula implies that the complex conjugate of $\hat{B}(-\Delta\mathbf{k}_\ell)$ equals $\hat{B}(\Delta\mathbf{k}_\ell)$. Then both the integrand and the increment process in (2) are Fourier transforms of the respective terms in (1). The restriction $0 < H < 1$ is also shown in the requirement that the integrand in (2) is square integrable, and the distributional equality of the two forms (1) and (2) is a result of the Parseval identity [cf. *Samorodnitsky and Taqqu*, 1994, proposition 7.2.7].

[11] The fractional Brownian field (1) can be simulated using discrete Fourier transforms. Using the spectral representation (2) we approximate $B_\varphi(\mathbf{x}) \approx \bar{B}_\varphi(\mathbf{x}) - \bar{B}_\varphi(\mathbf{0})$ where

$$\bar{B}_\varphi(\mathbf{x}) = \sum_\ell e^{i\mathbf{k}_\ell\cdot\mathbf{x}}\hat{\varphi}(\mathbf{k}_\ell)\hat{B}(\Delta\mathbf{k}_\ell), \tag{4}$$

which is evidently the inverse discrete Fourier transform of the product $\hat{\varphi}(\mathbf{k}_\ell)\hat{B}(\Delta\mathbf{k}_\ell)$. Then in order to simulate $\bar{B}_\varphi$ we can begin by simulating $B(\Delta\mathbf{y}_j)$ as iid random variables on a regular grid $\mathbf{y}_j$, take discrete Fourier transforms to obtain $\hat{B}(\Delta\mathbf{k}_\ell)$ on a regular grid $\mathbf{k}_\ell$, multiply by the Fourier filter $\hat{\varphi}(\mathbf{k}_\ell)$, and invert the discrete Fourier transform. Then we subtract the result at grid point $\mathbf{x} = \mathbf{y}_j$ from the result at grid point $\mathbf{x} = \mathbf{0}$ to obtain $B_\varphi(\mathbf{x}) \approx \bar{B}_\varphi(\mathbf{x}) - \bar{B}_\varphi(\mathbf{0})$. The discrete Fourier (and inverse Fourier) transforms can be efficiently computed using fast Fourier transforms. While we have described this simulation procedure for Gaussian random fields, a variety of stochastic integrals can be used, allowing a flexible and realistic tool for simulating K fields. For example, $\ln(K)$ increments at several field sites are well modelled by a Laplace distribution [*Meerschaert et al.*, 2004], which is essentially a double-sided exponential. A different method for simulating only Gaussian processes, starting in Fourier space [*Voss*, 1989; *Peitgen and Saupe*, 1988; *Gelhar*, 1993; *Ruan and McLaughlin*, 1998; *Dieker and Mandjes*, 2003] will not be pursued here.

[12] Although the stochastic (convolution) integral

$$\tilde{B}_\varphi(\mathbf{x}) = \int \varphi(\mathbf{x} - \mathbf{y})B(d\mathbf{y}) \tag{5}$$

does not exist because the function $\varphi(\mathbf{x} - \mathbf{y})$ is not square integrable, we can heuristically write $B_\varphi(\mathbf{x}) = \tilde{B}_\varphi(\mathbf{x}) - \tilde{B}_\varphi(\mathbf{0})$, the convergent difference of two divergent stochastic integrals. Since the form (5) represents a stationary process, the theory of linear filters can be applied, and it turns out that these filters correspond to certain fractional integrals. For a simple example, consider fractional Brownian motion (FBM) in one dimension. *Mandelbrot and van Ness* [1968] defined a one dimensional fractional Brownian motion (FBM) using

$$\tilde{B}_H(x) = \frac{1}{\Gamma(H + 1/2)}\int_{-\infty}^{x}(x - y)^{H-1/2}B(dy). \tag{6}$$

In this formulation, the stochastic integral depends only on the values of $B(dy)$ for $y < x$ (the past, if x represents time) and hence is termed "causal." When x represents a spatial variable, this restriction may not be needed, and *Mandelbrot* [1982] introduced a symmetric, bilateral version of FBM using

$$\tilde{B}_H(x) = \frac{1}{\Gamma(H + 1/2)}\int_{-\infty}^{\infty}|x - y|^{H-1/2}B(dy). \tag{7}$$

[13] The convolutions in (6) and (7) take values of $B(dy)$ and spread them according to the respective power law kernels. From the point of view of fractional calculus (see *Samko et al.* [1993] for a comprehensive exposition), these

integrals can be viewed as fractional-order integrals of the "white noise" $B(dy)$ [*Meyer et al.*, 1999; *Pipiras and Taqqu*, 2000; *Chechkin and Gonchar*, 2001]. Fractional derivatives and integrals are natural extensions of their integer-order counterparts, easily understood in terms of their Fourier transforms. Given a function $f(x)$ with Fourier transform $\hat{f}(k)$ and compact support (i.e., $f(x) = 0$ for $|x|$ large), it is well known that the nth derivative of $f(x)$ has Fourier transform $(ik)^n\hat{f}(k)$, and hence the n-fold integral has Fourier transform $(ik)^{-n}\hat{f}(k)$. Fractional derivatives and integrals replace the integer exponent n with a rational number α. A computation using generalized functions shows that $\Gamma(-\alpha)(ik)^{\alpha}$ is the Fourier transform of the function $x^{-1-\alpha}$ on $x > 0$ [*Samko et al.*, 1993]. Hence the α-order fractional derivative of $f(x)$ is the convolution of $f(x)$ with a power law:

$$\frac{d^{\alpha}f(x)}{dx^{\alpha}} = \frac{1}{\Gamma(-\alpha)}\int_{-\infty}^{x}(x-y)^{-\alpha-1}f(y)dy, \tag{8}$$

where this integral is to be understood in terms of generalized functions. If $\alpha < 0$ this formula defines a fractional integral of order $-\alpha$. Now the one-sided FBM formula (6) can be viewed as an $A = H + 1/2$ fractional integral of white noise. One also defines a negative-direction fractional derivative

$$\frac{d^{\alpha}f(x)}{d(-x)^{\alpha}} = \frac{1}{\Gamma(-\alpha)}\int_{x}^{\infty}(y-x)^{-\alpha-1}f(y)dy, \tag{9}$$

and then the two-sided FBM formula (7) is seen as a combination of positive- and negative-direction fractional integrals of white noise with the same order $A = H + 1/2$. Since $0 < H < 1$, this means that heuristically FBM can be written $B_H(x) = \tilde{B}_H(x) - \tilde{B}_H(0)$ where $\tilde{B}_H(x)$ is a white noise fractional integral of order $1/2 < A < 3/2$. One-sided FBM can be simulated using the Fourier filter $\hat{\varphi}(k) = (ik)^{-A}$ in (4). Two-sided FBM results from using the equally weighted forward and backward fractional integrals, hence the symmetric filter $\hat{\varphi}(k) = (ik)^{-A} + (-ik)^{-A} = 2\cos(A\pi/2)|k|^{-A}$ where again $A = H + 1/2$ is the order of fractional integration. Using the filter $\hat{\varphi}(k) = |k|^{-A}$ multiplies the resulting FBM by a constant.

[14] We note here that the causal function (6) was originally intended for time series, since the present cannot influence the past. A similar treatment, in multiple dimensions, must be considered for the deposition of sediment in supercritical flow, since a disturbance in the flow is not propagated upstream. Therefore a convolution kernel that mathematically transmits fluctuations in the K field should not necessarily have equal (or any) weight in certain directions. In one dimension, a simple extension of the symmetric kernel in formula (7) incorporates a weight function $M(\theta)$, where $\theta = \pm 1$: $\hat{\varphi}(k) = M(1)(ik)^{-A} + M(-1)(-ik)^{-A}$, where again, $A = H + 1/2$ is the order of fractional integration. This concept of weights on the unit circle extends to two and three dimensions (below). It is also worth noting here that the one-sided and symmetric FBM are models of different processes and have noticeably different traces, even though the correlation structure of the increments (i.e., the spectral density functions) are identical.

[15] Fractional Gaussian noise (FGN) $G_H(x) = B_H(x) - B_H(x-1)$ is the increment process of fractional Brownian motion; hence we can simulate one-sided FGN using the Fourier filter $\hat{\varphi}(k) = [1 - e^{-ik}](ik)^{-H-1/2}$ in (4). Using a Taylor series approximation we can simplify this to $\hat{\varphi}(k) = (ik)^{-H+1/2}$. Similarly we can simulate two-sided FGN using the filter $\hat{\varphi}(k) = |k|^{-A}$ where now $A = H - 1/2$. This extends the simulation procedure through the interval $-1/2 < A < 1/2$, where again A indicates the order of fractional integration. For simplicity, we will continue to use this notation, since using H becomes somewhat confusing when referring to both FGN and FBM.

[16] Symmetric FBM in one dimension is a special case of an isotropic Brownian random field. The d-dimensional isotropic version can be simulated using the Fourier filter $\hat{\varphi}(\mathbf{k}) = \|\mathbf{k}\|^{-H-d/2}$ in (4), which corresponds to (1) with $\varphi(\mathbf{x}) = C\|\mathbf{x}\|^{H-d/2}$ for some constant C depending only on H and the dimension d of the variable $\mathbf{x}$. A stretching of the random field, resulting in greater strength or weight of correlation of the increments in some direction, but still decaying with the same power law (i.e., the same Hurst coefficient in all directions), is achieved by a scalar multiplication of the orthogonal vector components in the Fourier filter [*Rajaram and Gelhar*, 1995; *Zhan and Wheatcraft*, 1996; *Di Federico et al.*, 1999]:

$$\hat{\varphi}(\mathbf{k}) = \|\lambda\cdot\mathbf{k}\|^{-A} = \left((\lambda_1 k_1)^2 + (\lambda_2 k_2)^2 + (\lambda_3 k_3)^2\right)^{-A/2}. \tag{10}$$

This approach does not address the possibility that the decay of statistical dependence in any direction may fall off according to a different power law. Hence, in contrast to previous researchers, we call this stretched version with scalar H "functionally isotropic," since the power law is the same except for a prefactor, in all directions. Real aquifers may show different fractal scaling properties in the horizontal direction than the vertical [*Hewitt*, 1986; *Molz and Boman*, 1993; *Liu and Molz*, 1996]. Other aquifer characteristics that may serve as surrogates to K, such as sonic velocity, may also show differences in the scaling exponent in the direction of strike versus dip [*Deshpande et al.*, 1997]. *Molz et al.* [1997] suggest a scheme to change the order of integration in one direction via an expression similar to:

$$\hat{\varphi}(\mathbf{k}) = \left((\lambda_1 k_1)^2 + (\lambda_2 k_2)^2 + |\lambda_3 k_3|^{2\beta}\right)^{-A/2}. \tag{11}$$

In a subsequent section, we investigate the scaling properties of the random field generated by this and more general anisotropically scaling filters.

[17] Finally, in many depositional environments, the degree of dependence and connectivity of high-K units may have strong directionality and/or causality. If the stretched isotropic filter (10) is represented in polar coordinates $\hat{\varphi}(r, \theta) = M(\theta)r^{-A}$, then the set of weights is a smooth ellipse with axes lengths given by λ_i^{-A}, clearly dissimilar to the shape measured in Figure 2. Even more compelling examples are given by fractured aquifers, which may have fractures restricted to a small number of preferred orientations in three dimensions. In the directions transverse to fracture sets, there may or may not be any correlation in the fracture spacing or point K values. In the fracture planes, however, the connectivity and long-range dependence of K values will be much larger. Only upon upscaling of suffi-

ciently dense fractures [*Snow*, 1964, 1969; *Long et al.*, 1982] can an equivalent porous medium with a K tensor be defined. In the case of fractal fracture networks, it is unclear whether a separation of scales exists that allows upscaling to an equivalent porous medium with the typical K tensor. Upon any upscaling, the flow may be dominated by just a few major fractures brought into the observation window.

[18] The isotropically scaling filter $\hat{\varphi}(\mathbf{k}) = \|\mathbf{k}\|^{-A}$ corresponds to multivariable fractional integration of order A, since multiplication by $\|\mathbf{k}\|^{A}$ in Fourier space is equivalent to taking the fractional Laplacian $\Delta^{A/2} = (\partial^2/\partial x^2 + \partial^2/\partial y^2 + \partial^2/\partial z^2)^{A/2}$ in real space [*Bojdecki and Gorostiza*, 1999]. Similarly, the filter (10) corresponds to the inverse of the operator $(\lambda_1^2\partial^2/\partial x^2 + \lambda_2^2\partial^2/\partial y^2 + \lambda_3^2\partial^2/\partial z^2)^{A/2}$ and (11) to the inverse of $(\lambda_1^2\partial^2/\partial x^2 + \lambda_2^2\partial^2/\partial y^2 + \lambda_3^2\partial^\beta/\partial|z|^\beta)^{A/2}$. These are three special cases of the general multivariable fractional derivative operator recently introduced by *Meerschaert et al.* [2001] to model anomalous diffusion, and applied to solute transport by *Schumer et al.* [2003a]. The general form of this operator allows the order of derivative, as well as the weight $M(\theta)$ that determines the strength, or prefactor, of the derivative, to vary with coordinate.

3. Analytic Predictions of Solute Transport in Monofractal *K* Fields

[19] *Kemblowski and Wen* [1993], *Neuman* [1995], *Rajaram and Gelhar* [1995], *Zhan and Wheatcraft* [1996], *Bellin et al.* [1996], and *Di Federico and Neuman* [1998] predict the rate of plume spreading through a fractal (typically FBM) K field on the basis of a single value of H in the direction of transport. Our numerical experiments (section 5) are most closely aligned with the assumptions of *Neuman* [1995], *Rajaram and Gelhar* [1995], and *Di Federico and Neuman* [1998], so we focus here on their results. *Neuman* [1995] and *Di Federico and Neuman* [1998] assume purely advective flow so that each particle stays within a stream tube whose velocity autocorrelation function then becomes a scaled copy of the K correlation function in the direction of transport. This assumption is based on low variance of the K field, since the flow will bypass low-K zones and focus through high-K zones to a greater degree as the variance grows, thereby allowing the solute particles to subsample the random K field.

[20] Making three additional and distinct assumptions, *Di Federico and Neuman* [1998] predict that the plume will grow either in an early preasymptotic (pre-ergodic), asymptotic (ergodic), or permanently preasympototic state. Their results depend primarily on the average travel distance of a plume relative to a large-scale (low-frequency) fractal cutoff in either the K field or the plume itself. An early preasymptotic plume may follow totally "unmixed" ballistic motion, similar to the stratified model described by *Mercado* [1967]. This earliest stage is characterized by linear growth of the ensemble particle trajectory standard deviation and macrodispersivity versus travel distance ($a_\ell \propto \bar{X}$). An asymptotic plume occurs when the plume has travelled a greater distance than the scale of the largest heterogeneity present. If the particles stop experiencing new scales of heterogeneity (either through truncation of the K field heterogeneity or by subsampling do to advective mixing) the plume will transition to an asymptotic, or Fickian, growth rate (a_L = constant). Finally, *Di Federico and Neuman* [1998] reason that a plume travelling in fractal material is continually sampling larger scales of heterogeneity that are, on average, the same size as the growing mean travel distance. Such a plume is permanently preasymptotic and has a longitudinal macrodispersivity (a_L) that grows according to [*Di Federico and Neuman*, 1998]:

$$a_L \equiv \frac{1}{2}\frac{d}{d\bar{X}}\mathrm{VAR}(X) \propto \bar{X}^{1+2H}, \tag{12}$$

where VAR(X) is the variance of the particle travel distance, $\bar{X}$ is the mean travel distance, and H refers to the Hurst coefficient in the direction of travel.

[21] If one assumes that particles are free to roam a domain with a fixed large-scale fractal cutoff (for example, a finite domain), then at early time the mean travel distance may be much smaller than both the possible particle trajectories (because of the large heterogeneity of the flow path velocities), and the large-scale K cutoff. Furthermore, as time progresses, and a plume grows around its mean position, the mean distance becomes smaller relative to the increasing proportion of large excursions, which dominate the plume variance. Hence the mean position may be much smaller than either the plume or K large-scale cutoff and the plume may be approximately "early preasymptotic". In any case (early preasymptotic, permanently preasymptotic, or asymptotic), *Di Federico and Neuman* [1998] predict the plume dynamics on the basis of only the Hurst coefficient in the direction of travel.

[22] *Rajaram and Gelhar* [1995] use a two-particle, relative dispersion approach to calculate the macrodispersivity in a plume-specific (not ensemble) manner that corresponds most closely to *Di Federico and Neuman*'s [1998] permanently preasymptotic results. *Rajaram and Gelhar* [1995] compute the macrodispersivity in an FBM K field with a single value of H as

$$a_L \propto \bar{X}^H. \tag{13}$$

[23] The common feature of the analytic results on transport through fractal porous media is the isotropic scaling according to a single scaling parameter H. *Liu and Molz* [1996] posit that a different H in the direction transverse to flow may influence transport, since lateral mixing is determined by the layered structure of the aquifer material. Larger values of A or H correspond to greater persistence of the random increments, hence thicker layering of similar material. The thicker, more extensive layers should contribute to less mixing and more Mercado-type [*Mercado*, 1967] (ballistic) dispersion. Less extensive layering, characteristic of smaller values of A or H, should promote more mixing and perhaps more Fickian-type dispersion. In section 5 we investigate *Liu and Molz'* [1996] forecast that knowledge of H in the direction of transport alone is inadequate to predict plume growth.

4. Operator-Scaling Random Fields

[24] A functionally isotropic fractional Brownian random field $B_H(\mathbf{x})$ in d dimensions results from applying the Fourier filter $\hat{\varphi}(\mathbf{k}) = \|\mathbf{k}\|^{-A}$ to a Gaussian white noise in the spectral representation (2), where the scalar exponent $A = H +$

$d/2$ is used. Using the scaling relations $\hat{\varphi}(c\mathbf{k}) = c^{-A}\hat{\varphi}(\mathbf{k})$ and $\hat{B}(cd\mathbf{k}) = c^{d/2}\hat{B}(d\mathbf{k})$ we get

$$\begin{aligned} B_H(c\mathbf{x}) &= \int \left[e^{ic\mathbf{k}\cdot\mathbf{x}} - 1\right]\hat{\varphi}(\mathbf{k})\hat{B}(d\mathbf{k}) \\ &= \int \left[e^{i\mathbf{k}\cdot\mathbf{x}} - 1\right]\hat{\varphi}(c^{-1}\mathbf{k})\hat{B}(c^{-1}d\mathbf{k}) \\ &= \int \left[e^{i\mathbf{k}\cdot\mathbf{x}} - 1\right]c^{A}\hat{\varphi}(\mathbf{k})c^{-d/2}\hat{B}(d\mathbf{k}), \end{aligned}$$

and the last integral equals $c^H B_H(\mathbf{x})$ since $H = A - d/2$. Hence the scaling property $B_H(c\mathbf{x}) = c^H B_H(\mathbf{x})$ also follows directly from the scaling of the Fourier filter. The stretched Fourier filter in (10) also satisfies $\hat{\varphi}(c\mathbf{k}) = c^{-A}\hat{\varphi}(\mathbf{k})$; hence the process (2) with this filter has the same scaling property $B_\varphi(c\mathbf{x}) = c^H B_\varphi(\mathbf{x})$ as a fractional Brownian field.

[25] The Fourier filter (11) proposed by *Molz et al.* [1997] has a more complicated scaling $\hat{\varphi}(ck_1, ck_2, c^{1/\beta}k_3) = c^{-A}\hat{\varphi}(\mathbf{k})$ most conveniently handled using matrix powers [see, e.g., *Meerschaert and Scheffler*, 2001, section 2.2]. The matrix power $c^{\mathbf{Q}}$ is defined by a Taylor series $[c^{\mathbf{Q}} = \exp(\mathbf{Q}\ln c) = \mathbf{I} + \mathbf{Q}\ln c + \frac{(\mathbf{Q}\ln c)^2}{2!} + \frac{(\mathbf{Q}\ln c)^3}{3!} + \cdots]$ where $\mathbf{I}$ is the $d \times d$ identity matrix. Using this notation, the scaling for the Fourier filter (11) can be written as $\hat{\varphi}(c^{\mathbf{Q}}\mathbf{k}) = c^{-A}\hat{\varphi}(\mathbf{k})$ where $\mathbf{Q}^{-1} = \mathrm{diag}(1, 1, \beta)$. In this respect, we see that the matrix $\mathbf{Q}$ denotes deviations from the overall order of integration A. Then the random field of *Molz et al.* [1997] satisfies

$$\begin{aligned} B_\varphi(c^{\mathbf{Q}}\mathbf{x}) &= \int \left[e^{ic^{\mathbf{Q}}\mathbf{k}\cdot\mathbf{x}} - 1\right]\hat{\varphi}(\mathbf{k})\hat{B}(d\mathbf{k}) \\ &= \int \left[e^{i\mathbf{k}\cdot\mathbf{x}} - 1\right]\hat{\varphi}(c^{-\mathbf{Q}}\mathbf{k})\hat{B}(c^{-\mathbf{Q}}d\mathbf{k}) \\ &= \int \left[e^{i\mathbf{k}\cdot\mathbf{x}} - 1\right]c^{A}\hat{\varphi}(\mathbf{k})|c^{-\mathbf{Q}}|^{\frac{1}{2}}\hat{B}(d\mathbf{k}), \end{aligned} \tag{14}$$

where $|c^{-\mathbf{Q}}| = c^{-1-1-1/\beta}$ is the determinant of the matrix $c^{-\mathbf{Q}}$. Hence this random field satisfies the scaling relation $B_\varphi(c^{\mathbf{Q}}\mathbf{x}) = c^{A-1-\frac{1}{2\beta}}B_\varphi(\mathbf{x})$. Recalling that $A = H + 3/2$ for a three-dimensional field, we can also write this in the form,

$$B_\varphi\left(cx_1, cx_2, c^{1/\beta}x_3\right) = c^{H+\frac{1}{2}-\frac{1}{2\beta}}B_\varphi(\mathbf{x})$$

which reduces to the familiar scaling for a fractional Brownian field if we take $\beta = 1$.

[26] A wide variety of multiscaling random fields can be obtained in this manner (using equation (2)), so long as the integrand in (13) is square integrable. Another suitable choice of Fourier filter yields a random field with $B_\varphi(c^{1/H_1}x_1, c^{1/H_2}x_2, c^{1/H_3}x_3) = cB_\varphi(\mathbf{x})$ so that a different Hurst index $0 < H_i < 1$ applies to each coordinate. For example, the random field of *Molz et al.* [1997] has Hurst coefficient $H_i = H + \frac{1}{2} - \frac{1}{2\beta}$ for coordinates $i = 1, 2$ and $H_3 = \beta\left(H + \frac{1}{2}\right) - \frac{1}{2}$. A more general form of the filter comes from the theory of multivariable fractional differentiation where the generalized fractional derivative of a suitable function $f(\mathbf{x})$ is defined as the inverse Fourier transform of $\psi(\mathbf{k})\hat{f}(\mathbf{k})$ and $\exp[-\psi(\mathbf{k})]$ is the Fourier transform of an operator stable density function [*Meerschaert et al.*, 2001]. Using an example from section 2, the unstretched, isotropic Laplacian operator has the Fourier symbol $\psi(\mathbf{k}) = \|\mathbf{k}\|^2$ corresponding to the Fourier transform of a zero mean multi-Gaussian density $\exp[-\|\mathbf{k}\|^2]$. The general form of the Fourier symbol $\psi(\mathbf{k})$, given by the Lévy representation [*Meerschaert and Scheffler*, 2001; *Schumer et al.*, 2003a] is somewhat complex, but for our purposes it suffices to note that this function always satisfies a matrix scaling relation $c\psi(\mathbf{k}) = \psi(c^{\mathbf{Q}}\mathbf{k})$. Then the filter corresponding to a fractional integration $\hat{\varphi}(\mathbf{k}) = \psi(\mathbf{k})^{-A}$, where $A = H + d/2$, scales according to $c^A\hat{\varphi}(\mathbf{k}) = \hat{\varphi}(c^{-\mathbf{Q}}\mathbf{k})$. Once again a change to polar coordinates splits the function into the weight function $M(\theta)$ and a scaling function $r^{\mathbf{Q}}$; however, since $\mathbf{Q}$ may specify a different power law in any direction, a modified polar coordinate system is needed. A procedure for calculating this filter is listed in the Appendix A.

4.1. Examples

[27] To illustrate the effect of the weight function alone, we generated several two-dimensional random fields (Figure 3) with identical "random" Gaussian input fields but with four different functions $M(\theta)$. The fields are all isotropic with respect to the scaling coefficient $H = 0.3$. These realizations are typical for this scaling parameter. The first field uses the measure estimated by the directions of the braided stream in Figure 1 without respect to flow direction (Figure 3a). We then assume that the K values can only be influenced by upstream perturbations by zeroing upstream weights and adding them to those in the downstream direction (Figure 3b). Finally, we approximate the measure using a classical elliptical stretching (Figure 3d) and a simple "cross" of four weights on the x and y axes (Figure 3c). The plots clearly show the effect of generalizing the description of weights. The "downstream" measure develops much more continuity in the x direction than any other measure, while the classical elliptical measure shows the least. The latter is due to the unavoidable and possibly unrealistic placement of convolution weight transverse to the prevailing stream flow direction. The simple four-point "cross" measure develops a random field (Figure 3c) that bears a closer resemblance to the "downstream" measure. In section 5, we use this simple "cross" measure to construct fields with operator scaling (H different in the transverse and longitudinal directions) to investigate the impact of transverse H values on plume migration.

[28] In general, the eigenvalues of the scaling matrix $\mathbf{Q}$, and the overall order of integration A, define the Hurst index in each coordinate. The eigenvectors of $\mathbf{Q}$ specify those coordinates, and the weight function $M(\theta)$ indicates the importance of each direction in determining the dependence structure. The primary scaling directions (eigenvectors of the matrix $\mathbf{Q}$) need not be orthogonal, and the various directions can be given unequal weight of overall correlation. Because of the multiple scaling directions, these fields have the property of "generalized scale invariance" [*Schertzer and Lovejoy*, 1989], but do not have the multiple scaling *dimensions* associated with multiplicative cascades [*Mandelbrot*, 1974; *Frisch and Parisi*, 1983; *Benzi et al.*, 1984; *Lovejoy and Schertzer*, 1985; *Gupta and Waymire*, 1990; *Boufadel et al.*, 2000; *Veneziano and Essiam*, 2003]. However, we note one serious consequence of the operator scaling relationship: In general, the random process is distributionally self-similar along *curves* in physical space (Figure 4) unless one samples along the eigenvectors of the scaling matrix $\mathbf{Q}$. Sampling the process along straight lines between the eigenvectors will not follow a single power law (for any measure), and the observed scaling (Hurst)

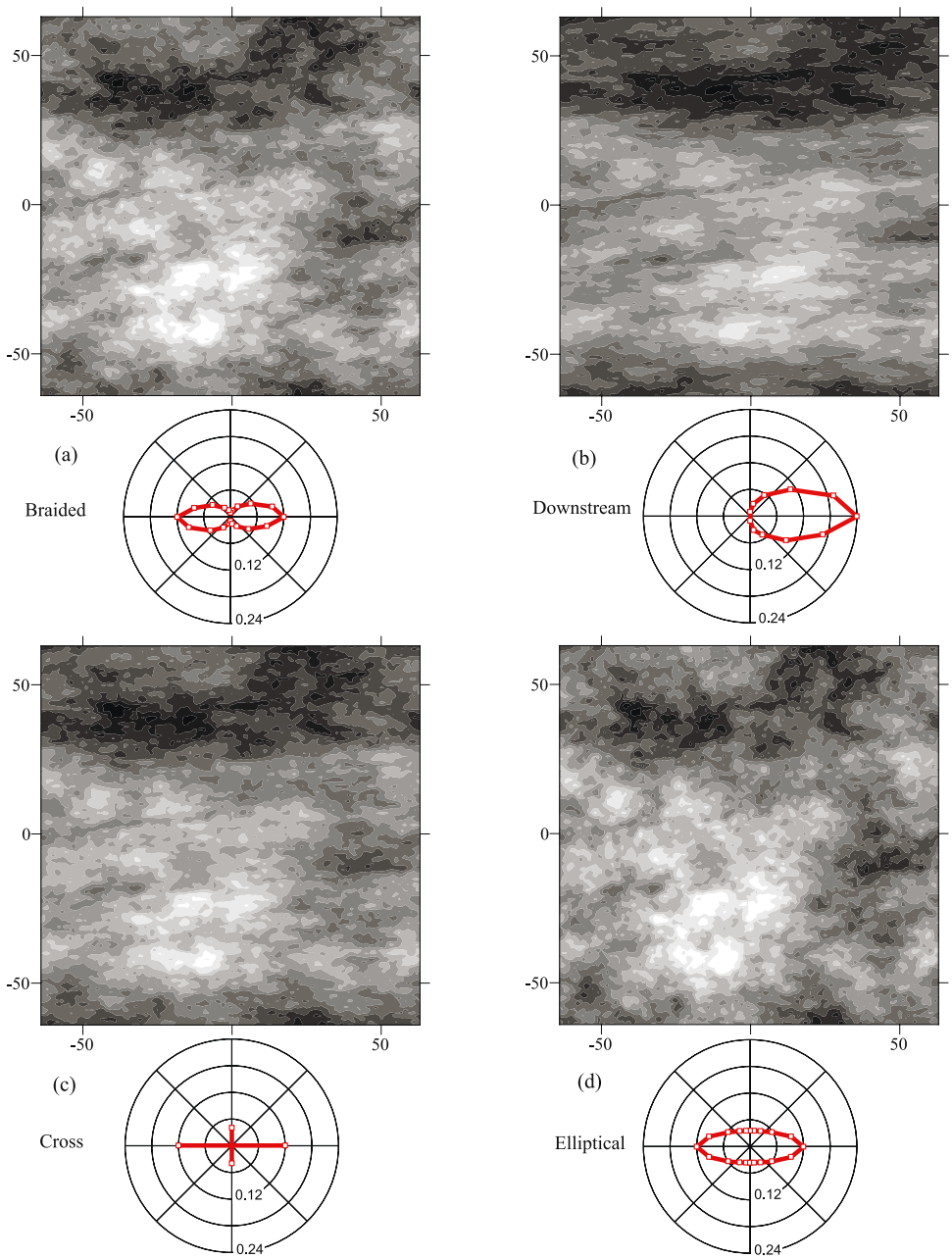

Figure 3. Effect of different weight functions $M(\theta)$, discretized at intervals of $\pi/10$ (polar plots), on isotropically scaling FBM (shaded plots): (a) measure estimated from braided stream directions, (b) downstream effects only, (c) simplified four-point measure, and (d) elliptical approximation. All weight functions are normalized to sum over θ to unity.

coefficient will change. For some measures used to distinguish multiplicative multifractals [see *Schertzer and Lovejoy*, 1987; *Boufadel et al.*, 2000; *Tennekoon et al.*, 2003], such as the structure function and spectral methods, the perceived fractal dimension will change unless care is first taken to find the eigenvectors of the scaling process.

[29] A closed form expression for $\psi(\mathbf{k})$ or $\hat{\varphi}(\mathbf{k})$ can only be written in certain instances. For a simple example of a filter that can be written in closed form, specify an order of integration A, and let the deviation matrix $\mathbf{Q}$ be diagonal in two dimensions with eigenvalues Q_1 and Q_2. Furthermore, let there be 4 weights on the unit circle of 0.45 on the $\pm x$ axis and 0.05 along the $\pm y$ axis. Then the orders of integration in the two coordinates are $A_1 = A/Q_1$ and $A_2 = A/Q_2$, and the kernel can be built from the Fourier symbol of the fractional derivative:

$$\psi(\mathbf{k}) = 0.45C_1\left((ik_1)^{1/Q_1} + (-ik_1)^{1/Q_1}\right) + 0.05C_2\left((ik_2)^{1/Q_2} + (-ik_2)^{1/Q_2}\right), \quad (15)$$

where $C_i = \Gamma(1 - 1/Q_i)$. A plot of $\hat{\varphi}(\mathbf{k}) = (\psi(\mathbf{k}))^{-A}$—the convolution kernel—with $A_1 = 1.2$ and $A_2 = 0.2$ (Figure 5) shows the different decay rates in the two directions and the discrete weights that transfer correlation in the chosen directions. In section 5, we use (15) to fractionally integrate

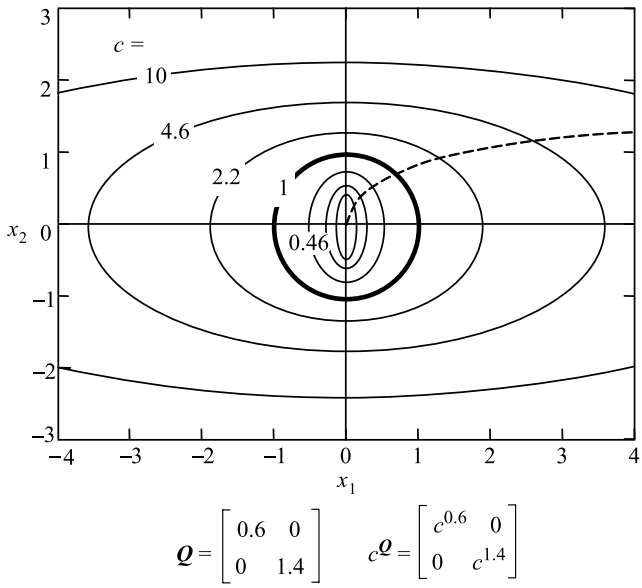

Figure 4. Ellipses of the operator rescaling of two-dimensional space $c^{\mathbf{Q}}\mathbf{x}$ for various rescaling values c and $\mathbf{Q}$ = diag(0.6, 1.4). The dashed line corresponds to the remapping of the point on the 45° angle for c = 1 (thick circle) onto other ellipses.

Gaussian noise and create a series of random fields, each with an identical A_1 but a different value of the parameter A_2. The resulting operator-fractional Gaussian fields are then used to investigate the effect of the order of aquifer scaling, transverse to mean flow, on contaminant migration.

[30] The possibility of nonorthogonal eigenvectors makes an operator-fractional field a good candidate for simulating physical properties of structurally deformed rock, since the fracture sets formed by stress relief are rarely orthogonal [e.g., *Davis*, 1984]. Presently, geostatistical simulation is used primarily to simulate undeformed sedimentary rock. Notable exceptions are *Ando et al.'s* [2003] nonparametric simulation of the densely fractured Fanay-AugPres site, and *Tsang et al.'s* [1996] sequential simulation and addition of fracture sets as an equivalent porous medium. In these studies, the scaling properties of the simulated fields were not fractal. In the latter study, individual fields were generated for each of the correlation structures and recombined, potentially altering the overall statistical properties of the fields. Using operator-fractional random fields, realistic self-similar permeability structures can be generated in one pass by varying the d principal scaling directions in d-dimensional space and their corresponding Hurst coefficients, as well as their relative weights.

[31] To illustrate, we chose two fracture sets (scaling eigenvectors) oriented $\pm\pi/8$ radians from the x axis. The weight function $M(\theta)$ is zero everywhere except for the $\pi/8$ and $7\pi/8$ directions (Figure 6, polar plots). Along those directions, the weights were made equal along both fracture sets (Figure 6, left), and three times greater on one of the fracture sets (Figure 6, right). The input uncorrelated noise (with no conditioning) was chosen to be Gaussian. The output field was normalized to have a standard deviation of 0.9 and exponentiated. The darker areas shown in Figure 6 are those with higher value of K. Note the fracture-like sparse and linear regions of connected high permeability. The positions of known fractures can be placed in the input noise, and the variability of effective K in individual fractures (or zones) is explicitly represented. Flow through such a limited "network" would strongly depend on both the scale of simulation and the specifics of both the weight function $M(\theta)$ and the fractal dimensions (power laws of the convolution) in various fracture directions. Such behavior is a hallmark of DFN simulations [e.g., *Bour and Davy*, 1998; *Bour et al.*, 2003; *Darcel et al.*, 2003a, 2003b; *de Dreuzy et al.*, 2004]. In a future study, we will investigate the correspondence of flow and transport through these random fields to DFN. In the next section, we investigate transport through operator-fractional granular aquifers and the applicability of monofractal analytic theories.

4.2. Field Evidence

[32] To motivate the numerical experiment in the next section, we reexamine the gas minipermeameter data that was collected near Escalante, Utah, and presented by *Castle et al.* [2004]. Point permeability data were collected along several horizontal and vertical transects in (1) an undisturbed upper shoreface cross-bedded sandstone and (2) an underlying bioturbated (disturbed) lower shoreface sandstone. The researchers calculated Hurst coefficients for a mixture of all horizontal transects (two in the disturbed and one in the undisturbed facies) and four vertical transects that span both facies. We calculated the rescaled range statistic (RS) for each horizontal line (with 110, 132, and 135 data points spaced 15 cm apart) and found that the lower two in the bioturbated facies do not show fractal structure. We assume that the extensive reworking of the sediments by burrowing animals altered any fractal structure that might have been present. Therefore we used only data from the upper cross-bedded unit, which left one horizontal and the upper portion of two vertical transects (with only 16 and 18 data points with spacing of 15 cm). While the vertical transects are severely shortened, the range statistics show reasonably fractal structure indicative of FBM with $H \approx 0.33$ over a small range (Figure 7a).

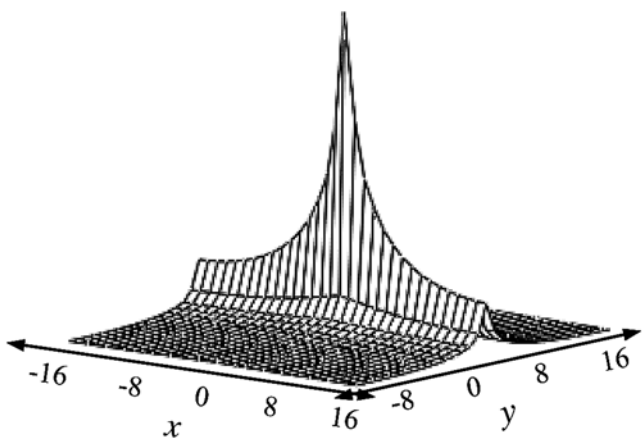

Figure 5. One possible convolution kernel leading to an operator-self-similar random process: two-dimensional kernel representing A_x = 1.2, A_y = 0.5 with total weights concentrated on the x and y axes of 0.9 and 0.1, respectively. Note both the slower decay due to a larger order of integration, and the greater convolution weight, in the x direction.

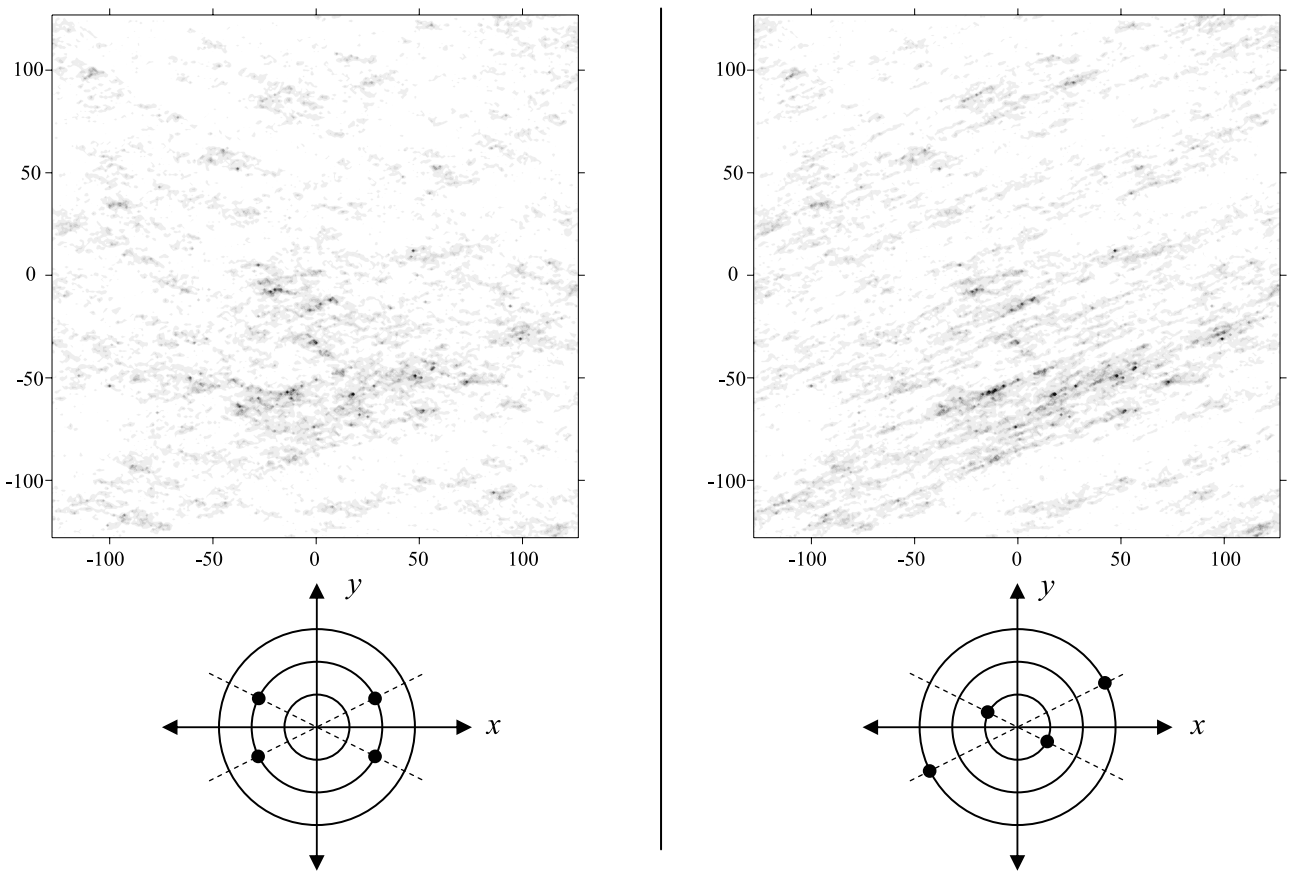

Figure 6. Operator-fractional Brownian fields (unconditional) for nonorthogonal scaling directions and weight functions. High K values are depicted by darker shading. The Hurst coefficient is isotropic with a value of $H = 0.3$. The dots on the polar plots illustrate the weights used in the upper simulations; that is, the right field has three times more weight along the $\pi/8$ radian direction.

[33] On the other hand, the horizontal RS plot shows fractal structure indicative of FBM with $H \approx 0.45$ over a wider range of scales (Figure 7a). The RS is only valid for larger lags [*Molz et al.*, 1997]. Dispersional analysis of the deviations of means taken over different partitions [*Caccia et al.*, 1997] is a less biased measure than the RS or variogram for FGN, and indicates slightly different structure—FBM with $H \approx 0.6$—at smaller partitions (Figure 7b). This points to either a multifractal structure, or that the measurement transects were not aligned with the principal scaling directions. One of the principal directions may, in fact, coincide with the cross beds [e.g., *Ritzi et al.*, 2004], which dip at low angle [*Castle et al.*, 2004]. Given the wide confidence intervals associated with the RS, and all other measures including the semivariogram and structure functions of various order [see, e.g., *Tennekoon et al.*, 2003], a number of different dependence models cannot be ruled out. For the purposes of our numerical experiment, we simply acknowledge that the statistics for this site support a model of $\ln(K)$ that is an operator-FBM with horizontal $H > 0.5$ and a lower H in the vertical. We have not attempted to find the principal directions of the scaling process.

[34] Numerous K measurements, like those from the Escalante site, very seldom are taken in the horizontal direction. One exception is *Desbarats and Bachu's* [1994] large-scale (up to 100 km) analysis of aquifer transmissivity, which is consistent with an FBM with $H \approx 0.26$. Further evidence for fractal K structure in the horizontal direction comes indirectly by inference from tracer data [*Neuman*, 1995; *Benson*, 1998]. Using the asymptotic assumption and (12) applied to apparent dispersivity data from a large number of sites, *Neuman* [1995] argues that H_{horiz} should be on the order of 0.25 for an FBM.

[35] More extensive vertical K data from boreholes have been analyzed to estimate the vertical Hurst coefficient [*Molz and Boman*, 1993; *Molz et al.*, 1997]. Very often, surrogate data are used to infer long-range dependence, such as gamma ray, spontaneous potential, or porosity logs from borehole geophysical surveys. Reported values of vertical H from a variety of these surrogates measured in sediments from various depositional environments span a very large range that includes both FGN and FBM [*Hewitt*, 1986; *Tubman and Crane*, 1995; *Pelletier and Turcotte*, 1996; *Deshpande et al.*, 1997]. The latter study also directly looked at the anisotropy of fractal structure of fluvial and deltaic sediments on the multikilometer scale using well logs and seismic reflection data. Using reflection amplitude from two planes extracted from distinct sandy horizons, they analyzed N-S and E-W transects for fractal structure. They concluded that the fluvial sediments (with high-amplitude channels trending north-northwest) in one horizontal plane were consistent with FBM with $H \approx 0.4$ to 0.65 in roughly the direction of channels (along dip) and

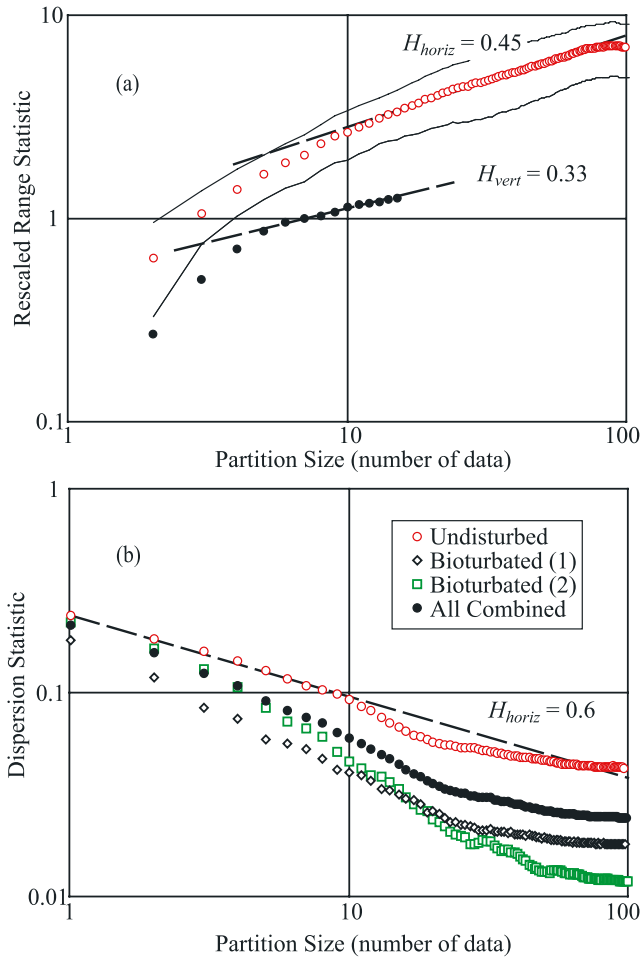

Figure 7. (a) Calculated range statistic (RS) from horizontal transect and portions of vertical transects within the undisturbed cross-bedded sandstone unit [*Castle et al.*, 2004]. The dashed lines indicate FBM in the transects with $H_{horiz} \approx 0.45$ and $H_{vert} \approx 0.33$. Solid lines indicate RS plus or minus one standard deviation. Note that for small lags, the RS is biased low, since it equals zero for lag 1. (b) Dispersion statistic (standard deviation of means) versus partition size for the horizontal transects.

$H \approx 0.05$ transverse to the channels (along strike). *Deshpande et al.* [1997] found less striking evidence of horizontal anisotropy in the deltaic sediments, with different H values of 0.26 versus 0.4. All of their vertical data was in the FBM range, with $H \approx 0.3$ to 0.5. To sum up the K and surrogate data from many studies using different data types and different scales, vertical measurement may show a large range of the order of integration, consistent with both FGN and FBM, while horizontal sediments typically are consistent with an FBM with $H \approx 0.25$ to 0.65. Also note that these studies do not always test the assumption that the increments are normally distributed. Many studies have shown that the K and/or ln K data from a particular site are distinctly non-Gaussian.

5. Solute Transport in Granular Aquifers

[36] To examine the effect of the difference of the Hurst coefficients in different directions, we conducted a numerical experiment. K fields were created that are identical in every way, except for the Hurst coefficient in the direction transverse to the mean flow. The fields were created using the same input Gaussian noise, so only the Fourier filter $\hat{\varphi}(\mathbf{k})$ was different. The two-dimensional Gaussian noise consisted of a 1024 $\times$ 1024 array of independent and identically distributed standard normal random variables. The noise was fast Fourier transformed, multiplied by the Fourier filter, and inverse fast Fourier transformed. The middle 1/4th of the field (now 512 $\times$ 512) was removed for flow and transport simulation.

[37] On the basis of the limited data in the horizontal direction, we specified an FBM with Hurst index of $H_1 = 0.7$ in the horizontal direction of flow, and varied the scaling index in the transverse direction, using orders of integration from $A_{vert} = 0.1$ to 1.5, signifying FGN with $H = 0.6$ up to an FBM with $H = 1.0$. Four of these fields are shown in Figure 8. The weights in the horizontal are equal left to right for a total of 0.9, versus similarly symmetric weight in the vertical of 0.1. For reference, when the vertical order of integration $A_{vert} = A_{horiz} = 1.2$, the field is similar to previous isotropic and stretched models of FBM [*Rajaram and Gelhar*, 1995; *Zhan and Wheatcraft*, 1996]. The only difference is our use of four discrete, rather than continuous (elliptical) weights. The output fields were adjusted to have zero mean and a standard deviation of 1.5, then exponentiated, so that each field is a lognormal operator-fractional field. The fields were tested for scaling properties in the two principal scaling directions by sampling all rows and columns from the field and applying both rescaled range and dispersional analyses [*Liu and Molz*, 1996; *Caccia et al.*, 1997]. These plots are not shown for brevity.

[38] After solving the head field using MODFLOW (assuming an average hydraulic gradient of 0.01 and no-flow boundaries on the top and bottom), particles were placed on the high-head side and tracked using *LaBolle et al.*'s [1996] particle tracking code. To make the simulations representative of real-world conditions, we included a small local dispersivity (equal in longitudinal and transverse directions) of 0.1 times the constant grid size of 0.3 m. Since this does not correspond exactly to *Neuman*'s [1995] and *Di Federico and Neuman*'s [1998] analytic results, we performed additional simulations with no local dispersion and found no noticeable differences. *Cushman* [1997] and *Hassan et al.* [1998] more fully discuss the influence of local and nonlocal fluxes on the accuracy of analytic methods in monofractal media.

[39] Increased orders of vertical integration (A_{vert}) have a distinct effect on both the simulated aquifer structure and the plume statistics. Lower values have less persistence of aquifer layers and allow (1) more advective mixing, (2) less spreading from persistent preferential flow, and (3) a transition from Mercado (ballistic) to Fickian flow (Figure 9). In contrast, as aquifer gains more vertical structure and layering from the increased order of integration, the plume spreads at a nearly Mercado-like (ballistic) rate over the entirety of the simulation. Even thought the mean and variance of the overall K distribution are exactly the same in all simulations, greater orders of transverse integration (A_{vert}) lead to thicker layers of high- and low-K material, hence more mass in the leading edge and trailing edges of the plume (Figure 10). The duration of breakthrough is greater by over an order of magnitude for the

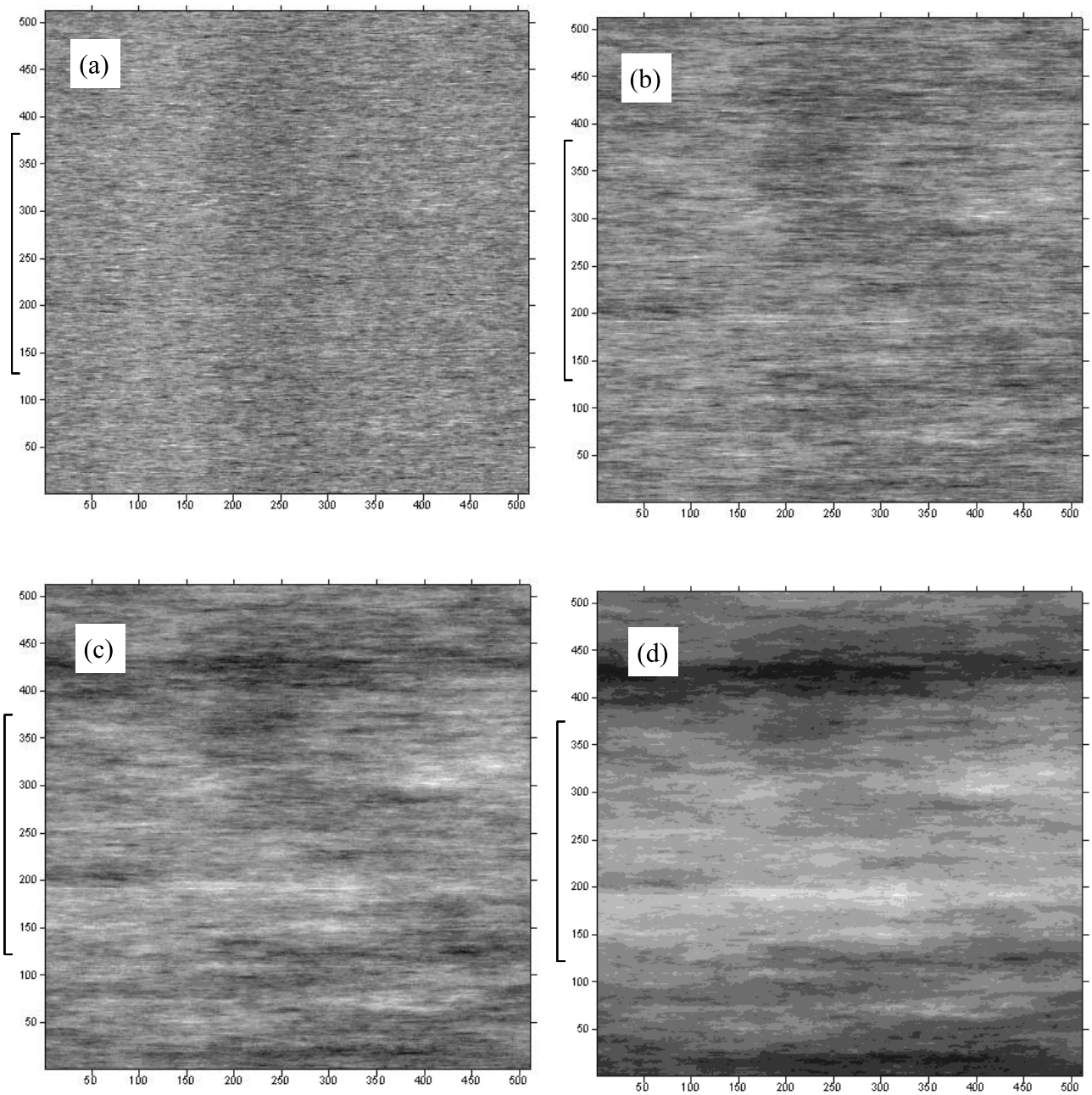

Figure 8. Shaded plots of four of the ln(K) fields. The fields are identical except for the order of vertical integration: (a) 0.1, (b) 0.5, (c) 0.9, and (d) 1.3. The fields are FBM in the horizontal direction with H = 0.7, or an order of integration A_{horiz} = 1.2. For particle tracking, 10,000 particles were released from the right side between nodes 128 and 384 (brackets).

most, versus least, layered aquifer. The contribution of early arrivals and late tailing are roughly equal. The lowest value of A_{vert} = 0.1 shows a near-Gaussian plume after 10,000 days (Figure 11a). The plumes become progressively less Gaussian and multimodal with greater transverse A_{vert}.

[40] Our numerical K fields have a low wave number cutoff equal to twice the domain size, since we subsampled the original 1024 × 1024 field. The Nyquist high wave number cutoff corresponds to the size of an individual cell. Therefore the mean positions of our numerical plumes are between the large and small cutoffs. According to the criteria of *Di Federico and Neuman* [1998], the plumes should be in a permanently preasymptotic state, where the apparent dipersivity should spread supralinearly (denoted by the steepest, solid line in Figure 9). The K fields should not foster asymptotic (Fickian) growth, if the assumptions inherent to the analytic theories are applicable. Since the elimination of local dispersion had negligible effect, we conclude that the transition to a Fickian regime by plumes in the aquifers with the least persistent layering is due primarily to advective mixing. The particles do not experience the exact K correlation structure in the longitudinal direction prescribed by the value of H_{horiz}, contrary to the assumption inherent to the analytic solutions [*Neuman*, 1995; *Di Federico and Neuman*, 1998; *Rajaram and Gelhar*, 1995]. The particles are free to "shortcut" between high-K zones

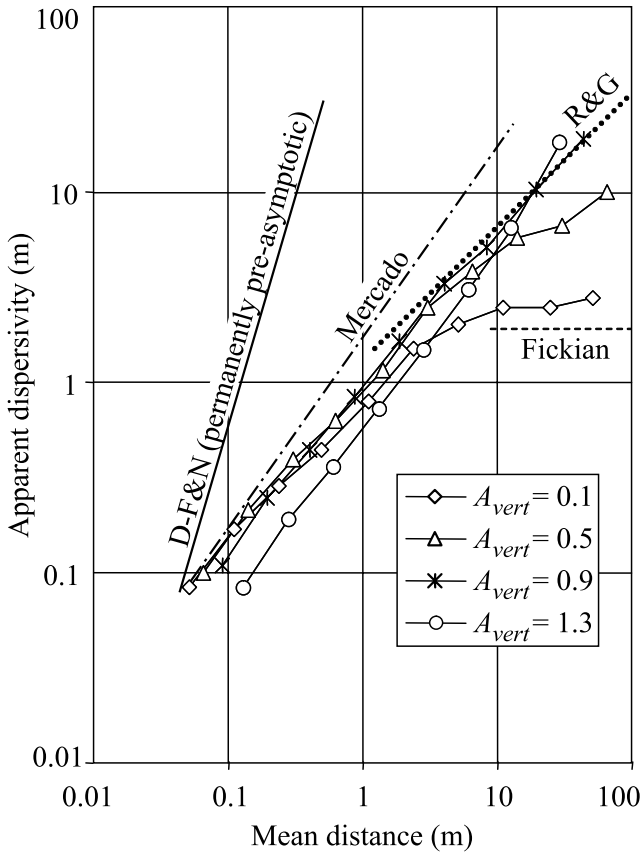

Figure 9. Apparent dispersivity versus mean particle distance for various orders of integration (A_{vert}) in the vertical direction. Solid and dash-dotted lines indicate permanently preasymptotic and early preasymptotic (i.e., Mercado) solutions, respectively, for monofractals [*Di Federico and Neuman*, 1998]. The dotted line indicates two-particle (single-plume) slope from *Rajaram and Gelhar* [1995]. The dashed line indicates Fickian motion.

and avoid the low-K zones, making the Lagrangian correlation structure different from the Eulerian K structure.

[41] Only the fields that are nearly monofractal, with A_{vert} = 0.9 and 1.3, agree qualitatively with the analytic predictions of *Rajaram and Gelhar* [1995] (Figure 9). In these cases the particles experience roughly the same Hurst coefficient along a trajectory no matter how much lateral mixing is taking place. Since these are single, not ensemble plumes, it is not surprising that Rajaram and Gelhar's two-particle predictions are more accurate in the nearly monofractal cases. However, these plumes are far from Gaussian in shape (Figures 11c and 11d). The plumes in the aquifers with the least persistent layering—with lower values of A_{vert} = 0.1 and 0.5—show convergence to a Fickian growth rate and an approximately Gaussian plume shape (Figures 10, 11a, and 11b), since we specified a finite variance lognormal K distribution. However, all of the plumes have significant fractions that travel well ahead of the Gaussian best fit (Figure 11). Because of the low ln(K) variance, none of the plumes show as much rapid transport in the leading edge as an α-stable plume undergoing fractional-order dispersion [*Benson et al.*, 2001]. One can expect that monofractally scaling fields with heavy-tailed, α-stable K increments can create even more rapid transport and α-stable plumes [*Herrick et al.*, 2002; *Grabasnjak*, 2003]; however, *Trefry et al.* [2003] show that lognormally distributed aquifers with exponential correlation decay may also engender highly channelized flow and α-stable growth behavior when both the integral scale and the variance of ln(K) are large.

[42] On the other end of the transport spectrum, the non-Fickian plumes (Figure 10) do not display the anomalous (power law) late-time tailing associated with fractal mobile/immobile and typical continuous time random walk formulations [*Berkowitz and Scher*, 1997; *Berkowitz et al.*, 2000; *Schumer et al.*, 2003b; *Dentz and Berkowitz*, 2003]. Since our VAR(ln K) was only 2.25 with a geometric mean of 0.3 m/d, the minimum K values were on the order of 10^{-4} m/d. This value is not low enough to make diffusion a dominant flux in our low-K zones [*Haggerty et al.*, 2000]. Had the variance of ln(K) been on the order of 4.0 or more, the presence of a fractal distribution of low-K zones, with flux dominated by diffusion, should induce this type of fractal delayed transport [*Haggerty et al.*, 2000].

[43] To summarize the results of the numerical experiment, we confirmed the fact that higher orders of integration in the vertical direction (corresponding to FBM with high H values) describe increased persistence of random values, hence greater layering or stratification. Plumes released in operator-fractional aquifers will spread at different rates, even with the same value of H in the direction of flow and identical ln(K) mean and variance. Those plumes in nearly monofractal aquifers plumes agree best with the monofractal analytic solution of *Rajaram and Gelhar* [1995], perhaps because their theory is developed for single, not ensemble plumes. A more extensive analysis of ensembles of operator-fractional plumes would be needed to confirm this. The breakthrough of plumes is drastically affected by the transverse scaling properties of the aquifer. The most stratified aquifer (FBM in the vertical with H = 0.8) had particles arrive nearly an order of magnitude before and after the least stratified aquifer. We used a simplistic measure of

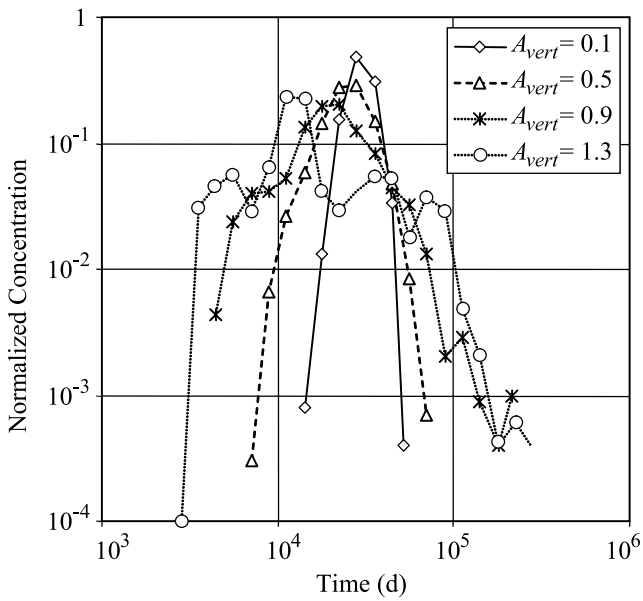

Figure 10. Breakthrough of particles at the boundary x = 156 m.

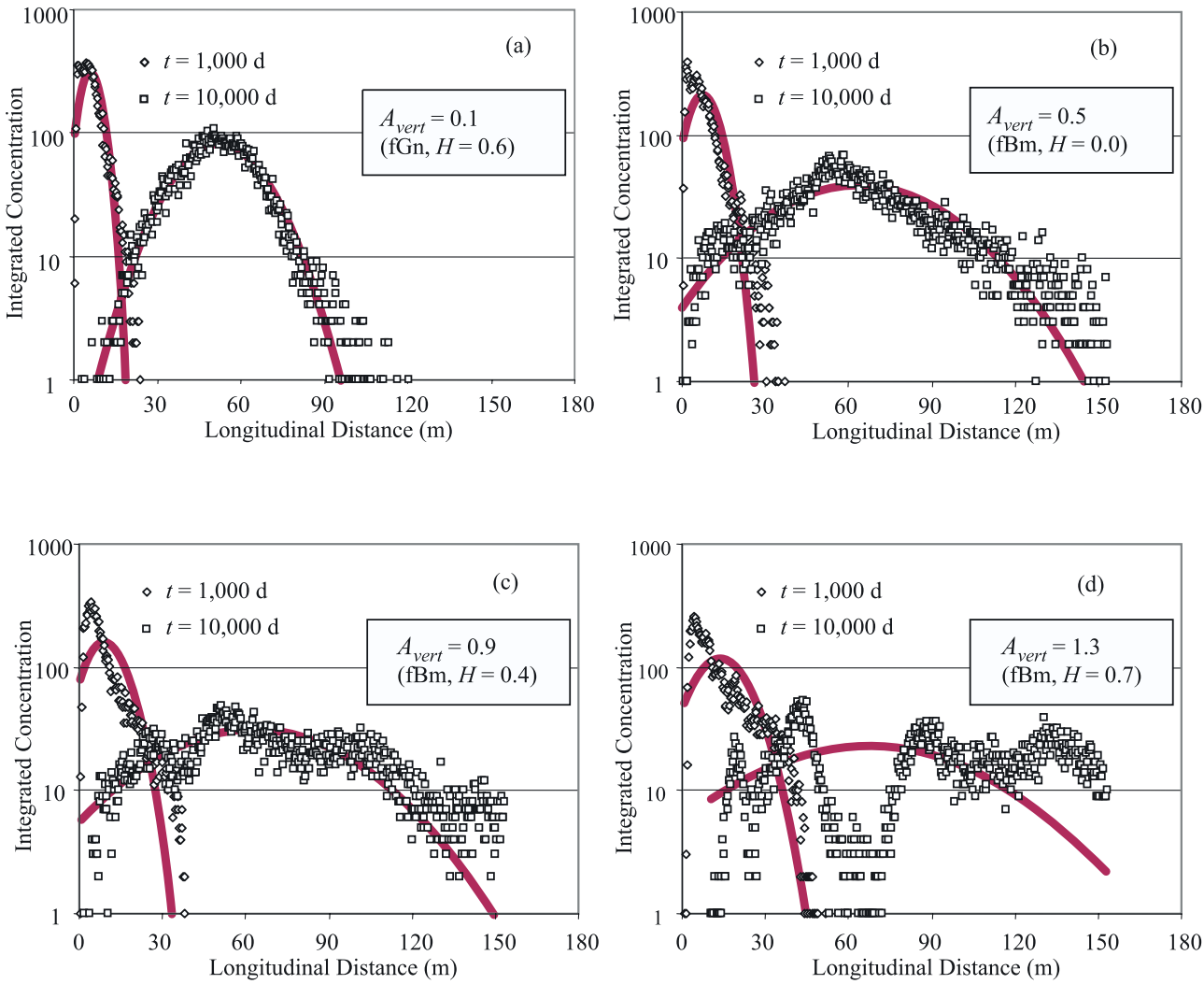

Figure 11. Semilog plots of vertically integrated concentration (plumes) versus longitudinal distance for the fields shown in Figure 8 with A_{vert} = [0.1, 0.5, 0.9, 1.3]. Best fit Gaussian curves underlie points.

directional K dependence in our approximation of a granular aquifer. Our measure of the directionality within the surface expression of a braided stream environment may show more complex structure and different plume mixing effects. We have not yet examined the effect of more complex directional measures $M(\theta)$, whether they represent granular (Figure 3) or fractured media (Figure 6).

6. Conclusions

[44] 1. A multidimensional operator-fractional Gaussian noise/Brownian motion, or combination of the two, can be created via Fourier transform by convolving an uncorrelated Gaussian noise with a function that has the correct matrix scaling relationship.

[45] 2. Many other distributions can be chosen for the uncorrelated noise in the numerical procedure, yielding a process with operator-self-similar increments. Furthermore, the input noise may be given nonstationary statistics to represent sequences of geologic material.

[46] 3. In d dimensions, the d primary scaling directions of the self-similar random field need not be orthogonal. Furthermore, the weights assigned to the directional fractional integrals, that is, the convolution kernel, are freely assigned to the d-dimensional unit sphere.

[47] 4. The longitudinal moments of a moving plume depend largely on the scaling (e.g., Hurst) coefficients in the directions transverse to flow. Prior analytic results do not account for this.

[48] 5. Smaller orders of integration, representing noise or motion with small Hurst coefficients, lead to less persistent aquifer layering and greater advective mixing of a plume. In contrast to previous analytic predictions, plumes in material with small orders of integration (i.e., noisy or less persistent layering) in the transverse direction may converge relatively quickly to Fickian-type transport, regardless of the K structure in the direction of transport.

Appendix A: Calculation of $\hat{\varphi}(\mathbf{k})$

[49] Recall that the Fourier filter $\hat{\varphi}(\mathbf{k}) = \psi(\mathbf{k})^{-A}$, where $A = H + d/2$ and $\psi(\mathbf{k})$ is the log characteristic function of some operator stable law with exponent $\mathbf{Q}$. It follows [e.g., *Jurek and Mason*, 1993] that $\psi(\mathbf{k})$ has the representation

$$\psi(\mathbf{k}) = \int_{\|\boldsymbol{\theta}\|=1} \int_0^\infty \left(e^{-i\mathbf{k}\cdot(r^{\mathbf{Q}}\boldsymbol{\theta})} - 1 - i\mathbf{k} \cdot \left(r^{\mathbf{Q}}\boldsymbol{\theta}\right) \right) \frac{dr}{r^2} \lambda(d\boldsymbol{\theta}) \quad \text{(A1)}$$

if the real parts of the eigenvalues of $\mathbf{Q}$ are in the interval (1/2, 1), whereas

$$\psi(\mathbf{k}) = \int_{\|\boldsymbol{\theta}\|=1} \int_0^\infty \left(e^{-i\mathbf{k}\cdot(r^{\mathbf{Q}}\boldsymbol{\theta})} - 1\right) \frac{dr}{r^2}\, \lambda(d\boldsymbol{\theta}) \qquad \text{(A2)}$$

if the real parts of the eigenvalues of $\mathbf{Q}$ are greater than one. In the following we will only consider the latter case. The first case can be dealt with similarly. The measure λ on the unit sphere is called the mixing measure or the spectral measure of ψ.

[50] Let $1 < a_1 \le a_2 \le \ldots \le a_d$ denote the real parts of the eigenvalues of $\mathbf{Q}$. Then $B_\varphi(\mathbf{x})$ defined by (2) exists, if $(d/2)(a_p - 1) < H < (d/2)(a_1 - 1) + a_1$ which is only possible if $a_d < (1 + 2/d)a_1$, putting some restriction on $\mathbf{Q}$. It follows that

$$B_\varphi\left(c^{\mathbf{Q}}\mathbf{x}\right) = c^{A - Tr(\mathbf{Q})/2} B_\varphi(\mathbf{x}) \qquad \text{(A3)}$$

in distribution, where $\mathrm{Tr}(\mathbf{Q})$ is the sum of the eigenvalues of $\mathbf{Q}$. Furthermore, the variance $V(\mathbf{x}) = \mathrm{VAR}(B_\varphi(\mathbf{x}))$ has the scaling relation $V(c^{\mathbf{Q}}\mathbf{x}) = c^{2A - \mathrm{Tr}(\mathbf{Q})} V(\mathbf{x})$. Note that in the isotropic fractional Brownian field case, corresponding to $\psi(\mathbf{k}) = \|\mathbf{k}\|$, we have $a_1 = a_d = 1$, so our condition in this special case reduces to the standard $0 < H < 1$ condition on H and (A3) is just $B_\varphi(c\mathbf{x}) = c^H B_\varphi(\mathbf{x})$.

[51] In order to compute $\psi(\mathbf{k})$ we use a discrete mixing measure $\lambda(d\theta) = \sum M(\theta_i)\delta_{\theta_i}$, a sum of point masses δ_{θ_i} with user-specified weights $M(\theta_i)$ (indicating the strength of the directional dependence). For a continuous measure $\lambda(d\theta)$ we use a discrete approximation.

[52] An important special case, generalizing the example in equation (15) can be obtained in the following way (we only describe the case $d = 2$, higher dimensional examples are obtained similarly): Fix any two nonparallel vectors θ_1 and θ_2 on the unit sphere and any two numbers $1 < a_1 < a_2 < 2a_1$. Pick any weights $M(\pm\theta_i)$ and define the spectral measure $\lambda(d\theta) = M(\theta_1)\delta_{\theta_1} + M(-\theta_1)\delta_{-\theta_1} + M(\theta_2)\delta_{\theta_2} + M(-\theta_2)\delta_{-\theta_2}$. Let $\mathbf{Q}$ be a 2×2-matrix with eigenvectors θ_1 and θ_2 and corresponding eigenvalues a_1 and a_2, respectively, so that $\mathbf{Q}\theta_i = a_i\theta_i$. Then, by some calculations we get from (A2) for some constants C_1, $C_2 > 0$ (only depending on a_1 and a_2) that

$$\psi(\mathbf{k}) = C_1\left(M(\theta_1)(i\mathbf{k}\cdot\theta_1)^{1/a_1} + M(-\theta_1)(-i\mathbf{k}\cdot\theta_1)^{1/a_1}\right) + C_2\left(M(\theta_2)(i\mathbf{k}\cdot\theta_2)^{1/a_2} + M(-\theta_2)(-i\mathbf{k}\cdot\theta_2)^{1/a_2}\right),$$

which corresponds to a weighted fractional derivative of order $1/a_1$ in direction $\pm\theta_1$ and of order $1/a_2$ in direction $\pm\theta_2$. If we let $\hat{\varphi}(\mathbf{k}) = \psi(\mathbf{k})^{-H-1}$ for some $a_2 - 1 < H < 2a_1 - 1$ then $B_\varphi(\mathbf{x})$ defined by (2) exists and scales as $B_\varphi(c^{\mathbf{Q}}\mathbf{x}) = c^{H+1-(a1+a2)/2} B_\varphi(\mathbf{x})$.

Notation

a_L	longitudinal dispersivity [L].
A	order of fractional integration.
$B(d\mathbf{x})$	uncorrelated (white) Gaussian noise.
$B_H(\mathbf{x})$	isotropic fractional Brownian motion.
$B_\varphi(\mathbf{x})$	(operator) fractional random field.
FBM	fractional Brownian motion.
d	number of dimensions.
H	Hurst coefficient.
$\mathbf{I}$	identity matrix.
$\mathbf{k}$	wave vector [L^{-1}].
K	hydraulic conductivity [LT^{-1}].
$M(\theta)$	measure of directional weight within $\varphi(\mathbf{x})$.
$\mathbf{Q}$	deviations from isotropy matrix.
VAR(Y)	variance of random variable Y.
$\bar{X}$	mean particle longitudinal travel distance.
θ	unit vector on the d-dimensional unit sphere.
$\varphi(\mathbf{x})$	scaling (convolution) kernel.
$\psi(\mathbf{k})$	log-characteristic function of operator-stable density.

[53] **Acknowledgments.** This work is supported by NSF grants DMS-0417869, DMS-0417972, DMS-0139927, DMS-0139943, EAR-9980484, and EAR-9980489 and U.S. DOE grant DE-FG03-98ER14885. We thank the two reviewers, Shlomo Neuman and Brian Wood, and the associate editor, John Selker, for excellent review comments.

References

Aban, I. B., M. M. Meerschaert, and A. K. Panorska (2006), Parameter estimation for the truncated Pareto distribution, *J. Am. Stat. Assoc.*, in press.

Adler, P. M., and J.-F. Thovert (1999), *Fractures and Fracture Networks*, Springer, New York.

Ando, K., A. Kostner, and S. P. Neuman (2003), Stochastic continuum modeling of flow and transport in a crystalline rock mass: Fanay-Augères, France, revisited, *Hydrogeol. J.*, *11*(5), 521–535.

Bechtel SAIC Company (BSC) (2004a), Technical basis document no. 2: Unsaturated zone flow, revision 1, Las Vegas, Nev. (Available at www.ocrwm.doe.gov/documents/43219_tbd/index.htm.)

Bechtel SAIC Company (BSC) (2004b), Technical basis document no. 10: Unsaturated zone transport, revision 1, Las Vegas, Nev. (Available at www.ocrwm.doe.gov/documents/43220_tbd/index.htm.)

Bellin, A., M. Pannone, A. Fiori, and A. Rinaldo (1996), On transport in porous formations characterized by heterogeneity of evolving scales, *Water Resour. Res.*, *32*(12), 3485–3496.

Benke, R., and S. Painter (2003), Modeling conservative tracer transport in fracture networks with a hybrid approach based on the Boltzmann transport equation, *Water Resour. Res.*, *39*(11), 1324, doi:10.1029/2003WR001966.

Benson, D. A. (1998), The fractional advection-dispersion equation: Development and application, Ph.D. thesis, Univ. of Nev., Reno.

Benson, D. A., R. Schumer, M. M. Meerschaert, and S. W. Wheatcraft (2001), Fractional dispersion, Lévy motion, and the MADE tracer tests, *Transp. Porous Media*, *42*, 211–240.

Benzi, R., G. Paladin, G. Parisi, and A. Vulpiani (1984), On the multifractal nature of fully developed turbulence and chaotic systems, *J. Phys. A Math. Gen.*, *17*, 3521–3531.

Berkowitz, B., and H. Scher (1997), Anomalous transport in random fracture networks, *Phys. Rev. Lett.*, *79*, 4038–4041.

Berkowitz, B., H. Scher, and S. E. Silliman (2000), Anomalous transport in laboratory-scale, heterogeneous porous media, *Water Resour. Res.*, *36*(1), 149–158.

Bodvarsson, G. S. (Ed.) (2003), Yucca Mountain, *J. Contam. Hydrol.*, *62–63*, 750 pp.

Bodvarsson, G. S., and Y. Tsang (Eds.) (1999), Yucca Mountain Project, *J. Contam. Hydrol.*, *38*, 1–425.

Bojdecki, T., and L. G. Gorostiza (1999), Fractional Brownian motion via fractional Laplacian, *Stat. Probab. Lett.*, *44*, 107–108.

Bonami, A., and A. Estrade (2003), Anisotropic analysis of some Gaussian models, *J. Fourier Anal. Appl.*, *9*(3), 215–236.

Bonnet, E., O. Bour, N. Odling, P. Davy, I. Main, P. Cowie, and B. Berkowitz (2001), Scaling of fracture systems in geological media, *Rev. Geophys.*, *39*(3), 347–384.

Boufadel, M., S. Lu, F. Molz, and D. Lavallee (2000), Multifractal scaling of the intrinsic permeability, *Water Resour. Res.*, *36*(11), 3211–3222.

Bour, O., and P. Davy (1998), On the connectivity of three-dimensional fault networks, *Water Resour. Res.*, *34*(10), 2611–2622.

Bour, O., P. Davy, J. de Dreuzy, and T. Le Borgne (2003), Stochastic models of fracture networks based on the broad-range fracture length distribution and the long-range fracture correlations, *Eos Trans. AGU*, *84*(46), Fall Meet. Suppl., Abstract H52B-03.

Bruining, J., D. vanBatenburg, L. W. Lake, and A. P. Yang (1997), Flexible spectral methods for the generation of random fields with power-law semivariograms, *Math. Geol.*, *29*(6), 823–848.

Burr, D., E. Sudicky, and R. Naff (1994), Nonreactive and reactive solute transport in three-dimensional heterogeneous porous media: Mean displacement, plume spreading, and uncertainty, *Water Resour. Res.*, *30*(3), 791–816.

Caccia, D. C., D. Percival, M. J. Cannon, G. Raymond, and J. B. Bassingthwaighte (1997), Analyzing exact fractal time series: Evaluating dispresional analysis and rescaled range methods, *Physica A*, *246*, 609–632.

Carle, S. F., and G. E. Fogg (1997), Modeling spatial variability with one- and multi-dimensional continuous Markov chains, *Math. Geol.*, *29*(7), 891–918.

Carrera, J., and L. Martinez-Landa (2000), Mixed discrete-continuum models: A summary of experiences in test interpretation and model predictions, in *Dynamics of Fluids in Fractured Rocks*, *Geophys. Monogr. Ser.*, vol. 122, edited by B. Fabyschenko, P. A. Witherspoon, and S. M. Benson, pp. 251–265, AGU, Washington, D. C.

Castle, J. W., F. J. Molz, S. Lu, and C. L. Dinwiddie (2004), Sedimentology and fractal-based analysis of permeability data, John Henry member, Straight Cliffs formation (upper Cretaceous), Utah, U.S.A., *J. Sediment. Res.*, *74*(2), 270–284.

Chechkin, A. V., and V. Y. Gonchar (2001), Fractional Brownian motion approximation based on fractional integration of a white noise, *Chaos*, *12*(2), 391–398.

Cushman, J. H. (1997), *The Physics of Fluids in Hierarchical Porous Media: Angstroms to Miles*, Springer, New York.

Cushman, J., B. Hu, and F. Deng (1995), Nonlocal reactive transport with physical and chemical heterogeneity: Localization errors, *Water Resour. Res.*, *31*(9), 2219–2238.

Cvetkovic, V., S. Painter, N. Outters, and J. O. Selroos (2004), Stochastic simulation of radionuclide migration in discretely fractured rock near the Äspö Hard Rock Laboratory, *Water Resour. Res.*, *40*, W02404, doi:10.1029/2003WR002655.

Darcel, C., O. Bour, and P. Davy (2003a), Stereological analysis of fractal fracture networks, *J. Geophys. Res.*, *108*(B9), 2451, doi:10.1029/2002JB002091.

Darcel, C., O. Bour, P. Davy, and J. R. de Dreuzy (2003b), Connectivity properties of two-dimensional fracture networks with stochastic fractal correlation, *Water Resour. Res.*, *39*(10), 1272, doi:10.1029/2002WR001628.

Davis, G. H. (1984), *Structural Geology of Rocks and Regions*, John Wiley, Hoboken, N. J.

de Dreuzy, J. -R., C. Darcel, P. Davy, and O. Bour (2004), Influence of spatial correlation of fracture centers on the permeability of two-dimensional fracture networks following a power law length distribution, *Water Resour. Res.*, *40*, W01502, doi:10.1029/2003WR002260.

Dentz, M., and B. Berkowitz (2003), Transport behavior of a passive solute in continuous time random walks and multirate mass transfer, *Water Resour. Res.*, *39*(5), 1111, doi:10.1029/2001WR001163.

Desbarats, A. J., and S. Bachu (1994), Geostatistical analysis of aquifier heterogeneity from the core scale to the basin scale: A case study, *Water Resour. Res.*, *30*(3), 673–684.

Deshpande, A., P. B. Flemings, and J. Huang (1997), Quantifying lateral heterogeneities in fluvio-deltaic sediments using three-dimensional reflection seismic data: Offshore Gulf of Mexico, *J. Geophys. Res.*, *102*(B7), 15,385–15,402.

Deutsch, C. V., and A. G. Journel (1992), *GSLIB: Geostatistical Software Library and User's Guide*, Oxford Univ. Press, New York.

Dieker, A. B., and M. Mandjes (2003), On spectral simulation of fractional Brownian motion, *Probab. Eng. Inf. Sci.*, *17*(3), 417–434.

Dietrich, C., and G. Newsam (1993), A fast and exact method for multidimensional Gaussian stochastic simulations, *Water Resour. Res.*, *29*(8), 2861–2870.

Dietrich, C., and G. Newsam (1996), A fast and exact method for multidimensional Gaussian stochastic simulations: Extension to realizations conditioned on direct and indirect measurements, *Water Resour. Res.*, *32*(6), 1643–1652.

Di Federico, V., and S. P. Neuman (1998), Transport in multiscale log conductivity fields with truncated power variograms, *Water Resour. Res.*, *34*(5), 963–974.

Di Federico, V., S. P. Neuman, and D. M. Tartakovsky (1999), Anisotropy, lacunarity, and upscaled conductivity and its autocovariance in multiscale random fields with truncated power variograms, *Water Resour. Res.*, *35*(10), 2891–2908.

Dobrushin, R. L. (1978), Automodel generalized random fields and their renorm group, in *Multicomponent Random Systems*, edited by R. L. Dobrushin and Y. G. Sanai, pp. 153–198, CRC Press, Boca Raton, Fla.

Eggleston, J., S. Rojstaczer, and J. Peirce (1996), Identification of hydraulic conductivity structure in sand and gravel aquifers: Cape Cod data set, *Water Resour. Res.*, *32*(5), 1209–1222.

Endo, H. K., J. C. S. Long, C. R. Wilson, and P. A. Witherspoon (1984), A model for investigating mechanical transport in fracture networks, *Water Resour. Res.*, *20*(10), 1390–1400.

Feyen, L., P. J. Ribeiro, Jr., F. De Smedt, and P. J. Diggle (2002), Bayesian methodology to stochastic capture zone determination: Conditioning on transmissivity measurements, *Water Resour. Res.*, *38*(9), 1164, doi:10.1029/2001WR000950.

Freeze, R. A. (1975), A stochastic-conceptual analysis of one-dimensional flow in nonuniform homogeneous media, *Water Resour. Res.*, *11*(5), 725–741.

Frisch, U., and G. Parisi (1983), On the singularity structure of fully developed turbulence, in *Turbulence and Predictability of Geophysical Flows and Climate Dynamics*, *Int. Sch. Phys. "Enrico Fermi"*, vol. 88, edited by M. Ghill, R. Benzi, and G. Parisi, pp. 84–88, Elsevier, New York.

Gelhar, L. W. (1993), *Stochastic Subsurface Hydrology*, Prentice-Hall, Upper Saddle River, N. J.

Gelhar, L. W., A. L. Gutjahr, and R. L. Naff (1979), Stochastic analysis of macrodispersion in a stratified aquifer, *Water Resour. Res.*, *15*(6), 1387–1397.

Grabasnjak, M. (2003), Random particle motion and fractional-order dispersion in highly heterogeneous aquifers, M.S. thesis, Univ. of Nev., Reno.

Graham, W., and D. McLaughlin (1989), Stochastic analysis of non-stationary subsurface solute transport: 2. Conditional moments, *Water Resour. Res.*, *25*(11), 2331–2355.

Guadagnini, A., and S. P. Neuman (1999a), Nonlocal and localized analyses of conditional mean steady state flow in bounded, randomly nonuniform domains: 1. Theory and computational approach, *Water Resour. Res.*, *35*(10), 2999–3018.

Guadagnini, A., and S. P. Neuman (1999b), Nonlocal and localized analyses of conditional mean steady state flow in bounded, randomly nonuniform domains: 2. Computational examples, *Water Resour. Res.*, *35*(10), 3019–3039.

Guadagnini, A., and S. P. Neuman (2001), Recursive conditional moment equations for advective transport in randomly heterogeneous velocity fields, *Transp. Porous Media*, *42*, 37–67.

Gupta, V., and E. Waymire (1990), Multiscaling properties of spatial rainfall and river flow distributions, *J. Geophys. Res.*, *95*(D3), 1999–2009.

Haggerty, R., S. A. McKenna, and L. C. Meigs (2000), On the late-time behavior of tracer test breakthrough curves, *Water Resour. Res.*, *36*(12), 3467–3479.

Hassan, A., J. Cushman, and J. Delleur (1997), Monte Carlo studies of flow and transport in fractal conductivity fields: Comparison with stochastic perturbation theory, *Water Resour. Res.*, *33*(11), 2519–2534.

Hassan, A. E., J. H. Cushman, and J. W. Delleur (1998), A Monte Carlo assessment of Eulerian flow and transport perturbation models, *Water Resour. Res.*, *34*(5), 1143–1163.

Hewitt, T. A. (1986), Fractal distribution of reservoir heterogeneity and their influence on fluid transport, paper presented at SPE 61st Annual Technical Conference and Exhibition, Soc. of Pet. Eng., New Orleans, La.

Herrick, M. G., D. A. Benson, M. M. Meerschaert, and K. R. McCall (2002), Hydraulic conductivity, velocity, and the order of the fractional dispersion derivative in a highly heterogeneous system, *Water Resour. Res.*, *38*(11), 1227, doi:10.1029/2001WR000914.

Hsieh, P. A., and S. P. Neuman (1985a), Field determination of the three-dimensional hydraulic conductivity tensor of anisotropic media: 1. Theory, *Water Resour. Res.*, *21*(11), 1655–1665.

Hsieh, P. A., S. P. Neuman, G. K. Stiles, and E. S. Simpson (1985b), Field determination of the three-dimensional hydraulic conductivity tensor of anisotropic media: 2. Methodology and application to fractured rocks, *Water Resour. Res.*, *21*(11), 1667–1676.

Hu, B., F. Deng, and J. Cushman (1995), Nonlocal reactive transport with physical and chemical heterogeneity: Linear nonequilibrium sorption with random K_d, *Water Resour. Res.*, *31*(9), 2239–2252.

Huang, H., and B. Hu (2001), Nonlocal reactive transport in heterogeneous dual-porosity media with rate-limited sorption and interregional mass diffusion, *Water Resour. Res.*, *37*(3), 639–648.

Huang, H., B. X. Hu, X.-H. Wen, and C. Shirley (2004), Stochastic inverse mapping of hydraulic conductivity and sorption partitioning coefficient fields conditioning on nonreactive and reactive tracer test data, *Water Resour. Res.*, *40*, W01506, doi:10.1029/2003WR002253.

Hudson, W., and J. D. Mason (1982), Operator-self-similar processes in a finite-dimensional space, *Trans. Am. Math. Soc.*, *273*, 281–297.

Hyun, Y., and S. P. Neuman (2003), Mono- and multi-fractal scalings of air permeability data from unsaturated fractured tuff, *Eos Trans. AGU*, *84*(46), Fall Meet. Suppl., Abstract H42B-1075.

Hyun, Y., S. P. Neuman, V. V. Vesselinov, W. A. Illman, D. M. Tartakovsky, and V. Di Federico (2002), Theoretical interpretation of a pronounced permeability scale effect in unsaturated fractured tuff, *Water Resour. Res.*, *38*(6), 1092, doi:10.1029/2001WR000658.

Jurek, Z. J., and J. D. Mason (1993), *Operator-Limit Distributions in Probability Theory*, John Wiley, Hoboken, N. J.

Kemblowski, M., and J. Wen (1993), Contaminant spreading in stratified soils with fractal permeability distribution, *Water Resour. Res.*, *29*(2), 419–426.

Kumar, P., and E. Foufoula-Georgiou (1993), A multi-component decomposition of spatial rainfall fields: 2. Self-similarity in fluctuations, *Water Resour. Res.*, *29*(8), 2533–2544.

LaBolle, E., G. Fogg, and A. F. B. Tompson (1996), Random-walk simulation of transport in heterogeneous porous media: Local mass-conservation problem and implementation methods, *Water Resour. Res.*, *32*(3), 583–594.

Li, S. G., and D. B. McLaughlin (1991), A nonstationary spectral method for solving stochastic groundwater problems: 1. Unconditional analysis, *Water Resour. Res.*, *27*(7), 1589–1605.

Li, S. G., D. McLaughlin, and H. S. Liao (2003), A computationally practical method for stochastic groundwater modeling, *Adv. Water Resour.*, *26*, 1137–1148.

Li, S. G., H. S. Liao, and C. F. Ni (2004), Stochastic modeling of complex nonstationary groundwater systems, *Adv. Water Resour.*, *27*, 1087–1104.

Liu, H., and F. Molz (1996), Discrimination of fractional Brownian movement and fractional Gaussian noise structures in permeability and related property distributions with range analyses, *Water Resour. Res.*, *32*(8), 2601–2606.

Liu, H., and F. Molz (1997), Multifractal analyses of hydraulic conductivity distributions, *Water Resour. Res.*, *33*(11), 2483–2488.

Long, J. C. S., J. S. Remer, C. R. Wilson, and P. A. Witherspoon (1982), Porous-media equivalents for networks of discontinuous fractures, *Water Resour. Res.*, *18*(3), 645–658.

Lovejoy, S., and D. Schertzer (1985), Generalized scale invariance in the atmosphere and fractal models of rain, *Water Resour. Res.*, *21*(8), 1233–1250.

Lu, S. L., F. J. Molz, and H. H. Liu (2003), An efficient, three-dimensional, anisotropic, fractional Brownian motion and truncated fractional Lévy motion simulation algorithm based on successive random additions, *Comput. Geosci.*, *29*(1), 15–25.

Mandelbrot, B. B. (1974), Intermittent turbulence in self-similar cascades: Divergence of high moments and dimension of the carrier, *J. Fluid Mech.*, *62*, 331–358.

Mandelbrot, B. B. (1982), *The Fractal Geometry of Nature*, W. H. Freeman, San Francisco, Calif.

Mandelbrot, B. B., and J. W. van Ness (1968), Fractional Brownian motion, fractional noises, and applications, *SIAM Rev.*, *10*, 422–437.

Martinez-Landa, L., and J. Carrera (2005), An analysis of hydraulic conductivity scale effects in granite (Full-scale Engineered Barrier Experiment (FEBEX), Grimsel, Switzerland), *Water Resour. Res.*, *41*, W03006, doi:10.1029/2004WR003458.

Mason, J. D., and Y. M. Xiao (2001), Sample path properties of operator-self-similar Gaussian random fields, *Theory Probab. Appl.*, *46*(1), 58–78.

Meerschaert, M. M., and H.-P. Scheffler (2001), *Limit Theorems for Sums of Independent Random Vectors*, John Wiley, Hoboken, N. J.

Meerschaert, M. M., D. A. Benson, and B. Baeumer (2001), Operator Lévy motion and multiscaling anomalous diffusion, *Phys. Rev. E*, *63*(2), 021112.

Meerschaert, M. M., T. J. Kozubowski, F. J. Molz, and S. Lu (2004), Fractional Laplace model for hydraulic conductivity, *Geophys. Res. Lett.*, *31*, L08501, doi:10.1029/2003GL019320.

Mercado, A. (1967), The spreading pattern of injected water in a permeability-stratified aquifer, *Int. Assoc. Sci. Hydrol. Publ.*, *72*, 23–36.

Meyer, Y., F. Sellan, and M. S. Taqqu (1999), Wavelets, generalized white noise and fractional integration: The synthesis of fractional Brownian motion, *J. Fourier Anal. Appl.*, *5*(5), 465–494.

Molz, F., and G. Boman (1993), A fractal-based stochastic interpolation scheme in subsurface hydrology, *Water Resour. Res.*, *29*(11), 3769–3774.

Molz, F., H. Liu, and J. Szulga (1997), Fractional Brownian motion and fractional Gaussian noise in subsurface hydrology: A review, presentation of fundamental properties, and extensions, *Water Resour. Res.*, *33*(10), 2273–2286.

Morse, B. S., G. Pohll, J. Huntington, and R. Rodriguez Castillo (2003), Stochastic capture zone analysis of an arsenic-contaminated well using the generalized likelihood uncertainty estimator (GLUE) methodology, *Water Resour. Res.*, *39*(6), 1151, doi:10.1029/2002WR001470.

Neuman, S. P. (1995), On advective transport in fractal permeability and velocity fields, *Water Resour. Res.*, *31*(6), 1455–1460.

Neuman, S. P. (2005a), Trends, prospects and challenges in quantifying flow and transport through fractured rocks, *Hydrogeol. J.*, *13*(1), 124–147.

Neuman, S. P. (2005b), On the tensorial nature of advective porosity, *Adv. Water Resour.*, *28*, 149–159.

Neuman, S. P., and V. Di Federico (2003), Multifaceted nature of hydrogeologic scaling and its interpretation, *Rev. Geophys.*, *41*(3), 1014, doi:10.1029/2003RG000130.

Neuman, S. P., G. R. Walter, H. W. Bentley, J. J. Ward, and D. D. Gonzalez (1984), Determination of horizontal aquifer anisotropy with three wells, *Ground Water*, *22*(1), 66–72.

Outters, N., and D. Shuttle (2000), Sensitivity analysis of a discrete fracture network model for performance assessment of Aberg, *Rep. 00-48*, Swed. Nucl. Fuel Waste Manage. Co., Stockholm.

Painter, S. (1996), Evidence for non-Gaussian scaling behavior in heterogeneous sedimentary formations, *Water Resour. Res.*, *32*(5), 1183–1196.

Painter, S. (2001), Flexible scaling model for use in random field simulation of hydraulic conductivity, *Water Resour. Res.*, *37*(5), 1155–1164.

Painter, S., and G. Mahinthakumar (1999), Prediction uncertainty for tracer migration in random heterogeneities with multifractal character, *Adv. Water Resour.*, *23*, 49–57.

Painter, S., and L. Paterson (1994), Fractional Lévy motion as a model for spatial variability in sedimentary rock, *Geophys. Res. Lett.*, *21*(25), 2857–2860.

Peitgen, H.-O., and D. Saupe (Eds.) (1988), *The Science of Fractal Images*, Springer, New York.

Pelletier, J. D., and D. L. Turcotte (1996), Scale-invariant topography and porosity variations in fluvial sedimentary basins, *J. Geophys. Res.*, *101*(B12), 28,165–28,176.

Pipiras, V., and M. S. Taqqu (2000), Integration questions related to fractional Brownian motion, *Probab. Theory Appl.*, *118*, 251–291.

Pipiras, V., and M. S. Taqqu (2003), Fractional calculus and its connections to fractional Brownian motion, in *Long-range Dependence: Theory and Applications*, edited by P. Doukhan, G. Oppenhain, and M. S. Taqqu, pp. 165–201, Springer, New York.

Rajaram, H., and L. Gelhar (1995), Plume-scale dependent dispersion in aquifers with a wide range of scales of heterogeneity, *Water Resour. Res.*, *31*(10), 2469–2482.

Rasmussen, T., D. Evans, P. Sheets, and J. Blanford (1993), Permeability of Apache Leap Tuff: Borehole and core measurements using water and air, *Water Resour. Res.*, *29*(7), 1997–2006.

Ritzi, R. W., Z. Dai, D. F. Dominic, and Y. N. Rubin (2004), Spatial correlation of permeability in cross-stratified sediment with hierarchical architecture, *Water Resour. Res.*, *40*, W03513, doi:10.1029/2003WR002420.

Robin, M., A. Gutjahr, E. Sudicky, and J. Wilson (1993), Cross-correlated random field generation with the direct Fourier transform method, *Water Resour. Res.*, *29*(7), 2385–2398.

Ruan, F., and D. McLaughlin (1998), An efficient multi-variate random field generator using the Fourier transform, *Adv. Water Resour.*, *21*, 385–399.

Samko, S. G., A. A. Kilbas, and O. I. Marichev (1993), *Fractional Integrals and Derivatives: Theory and Applications*, 976 pp., Gordon and Breach, New York.

Samorodnitsky, G., and M. Taqqu (1994), *Stable Non-Gaussian Random Processes*, CRC Press, Boca Raton, Fla.

Sapozhnikov, V., and E. Foufoula-Georgiou (1996), Self-affinity in braided rivers, *Water Resour. Res.*, *32*(5), 1429–1440.

Schertzer, D., and S. Lovejoy (1985), Generalised scale invariance in turbulent phenomena, *Phys. Chem. Hydrodyn. J.*, *6*, 623–635.

Schertzer, D., and S. Lovejoy (1987), Physically based rain and cloud modeling by anisotropic, multiplicative turbulent cascades, *J. Geophys. Res.*, *92*(D8), 9693–9714.

Schertzer, D., and S. Lovejoy (1989), Generalized scale invariance and multiplicative processes in the atmosphere, *Pure Appl. Geophys.*, *130*, 57–81.

Schumer, R., D. A. Benson, M. M. Meerschaert, and B. Baeumer (2003a), Multiscaling fractional advection-dispersion equations and their solutions, *Water Resour. Res.*, *39*(1), 1022, doi:10.1029/2001WR001229.

Schumer, R., D. A. Benson, M. M. Meerschaert, and B. Baeumer (2003b), Fractal mobile/immobile solute transport, *Water Resour. Res.*, *39*(10), 1296, doi:10.1029/2003WR002141.

Swedish Nuclear Fuel and Waste Management Company (SKB) (2001), RD&D programme 2001, *Tech. Rep. TR-01-30*, Stockholm. (Available at http://www.skb.se/upload/publications/pdf/TR-01-30.pdf.)

Smith, L., and F. W. Schwartz (1980), Mass transport: 1. A stochastic analysis of macroscopic dispersion, *Water Resour. Res.*, *16*(2), 303–313.

Snow, D. T. (1964), A parallel plate model of fractured permeable media, Ph.D. dissertation, 331 pp., Univ. of Calif., Berkeley.

Snow, D. T. (1969), Anisotropic permeability of fractured media, *Water Resour. Res.*, *5*(6), 1273–1289.

Stigsson, M., N. Outters, and J. Hermanson (2000), Äspö Hard Rock Laboratory, prototype repository hydraulic DFN model 2, *IPR 01-39*, Swed. Nucl. Fuel Waste Manage. Co., Stockholm.

Tennekoon, L., M. C. Boufadel, D. Lavallee, and J. Weaver (2003), Multifractal anisotropic scaling of the hydraulic conductivity, *Water Resour. Res.*, *39*(7), 1193, doi:10.1029/2002WR001645.

Tompson, A., and L. Gelhar (1990), Numerical simulation of solute transport in three-dimensional, randomly heterogeneous porous media, *Water Resour. Res.*, *26*(10), 2541–2562.

Tompson, A., R. Ababou, and L. Gelhar (1989), Implementation of the three-dimensional turning bands random field generator, *Water Resour. Res.*, *25*(10), 2227–2243.

Trefry, M. G., F. P. Ruan, and D. McLaughlin (2003), Numerical simulations of preasymptotic transport in heterogeneous porous media: Departures from the Gaussian limit, *Water Resour. Res.*, *39*(3), 1063, doi:10.1029/2001WR001101.

Tsang, Y., C. Tsang, F. Hale, and B. Dverstorp (1996), Tracer transport in a stochastic continuum model of fractured media, *Water Resour. Res.*, *32*(10), 3077–3092.

Tubman, K. M., and S. D. Crane (1995), Vertical versus horizontal well log variability and application to fractal reservoir modeling, in *Fractals in Petroleum Geology and Earth Processes*, edited by C. C. Barton and P. R. La Pointe, pp. 279–293, Springer, New York.

Veneziano, D., and A. K. Essiam (2003), Flow through porous media with multifractal hydraulic conductivity, *Water Resour. Res.*, *39*(6), 1166, doi:10.1029/2001WR001018.

Voss, R. F. (1989), Random fractals—Self-affinity in noise, music, mountains, and clouds, *Physica D*, *38*, 362–371.

Wellman, T. P., and E. P. Poeter (2005), Estimating spatially variable representative elementary scales in fractured architecture using hydraulic head observations, *Water Resour. Res.*, *41*, W03001, doi:10.1029/2004WR003287.

Wood, B. D., F. Cherblanc, M. Quintard, and S. Whitaker (2003), Volume averaging for determining the effective dispersion tensor: Closure using periodic unit cells and comparison with ensemble averaging, *Water Resour. Res.*, *39*(8), 1210, doi:10.1029/2002WR001723.

Woodbury, A., and T. Ulrych (2000), A full-Bayesian approach to the groundwater inverse problem for steady state flow, *Water Resour. Res.*, *36*(8), 2081–2094.

Yaglom, A. M. (1987), *Correlation Theory of Stationary and Related Random Functions*, vol. 1, Springer, New York.

Ye, M., S. P. Neuman, A. Guadagnini, and D. M. Tartakovsky (2004), Nonlocal and localized analyses of conditional mean transient flow in bounded, randomly heterogeneous porous media, *Water Resour. Res.*, *40*, W05104, doi:10.1029/2003WR002099.

Zhan, H., and S. W. Wheatcraft (1996), Macrodispersivity tensor for nonreactive solute transport in isotropic and anisotropic fractal porous media: Analytical solutions, *Water Resour. Res.*, *32*(12), 3461–3474.

B. Baeumer and M. M. Meerschaert, Department of Mathematics and Statistics, University of Otago, Dunedin 9001, New Zealand. (bbaeumer@maths.otago.ac.nz; mcubed@maths.otago.ac.nz)

D. A. Benson, Geology and Geological Engineering, Colorado School of Mines, 1500 Illinois St., Golden, CO 80401, USA. (dbenson@mines.edu)

H.-P. Scheffler, Department of Mathematics and Statistics, University of Nevada, Reno, NV 89512, USA. (pscheff@unr.edu)